Dysregulated Levels of TLRs, Cytokines and Chemokines in mouse brain infected with Japanese encephalitis virus via intracerebral route and tail vein route showing worst disease outcome

Shukla Mukti[1,2], Garg Atul[2], Dhole T.N.[2] and Chaturvedi Rachna[1*]
1. Amity Institute of Biotechnology, Amity University Uttar Pradesh, Lucknow Campus, 226028, INDIA
2. Sanjay Gandhi Post-Graduate Institute of Medical Sciences, Lucknow, 226014, INDIA
*rchaturvedi1@lko.amity.edu

Abstract

Despite the availability of vaccines, Japanese encephalitis (JE) is the leading cause of viral encephalitis related death each year in South East Asian region. As there is incomplete understanding on the pathogenesis of Japanese encephalitis virus (JEV), thousands of deaths are reported annually due to JEV infection in these regions. JEV also causes high morbidity in humans, leading to permanent neurological deficits, even in those who survive. In our recent research study[45], we explored the role of specific cytokines, chemokines and TLRs through in vitro studies. We demonstrated that exaggerated levels of TLRs (2,4 &9), cytokines (IL-6, IL-17 and chemokines (MCP-1, RANTES) in BV2 and Neuro2A cell lines were associated with worst outcome[45].

In present manuscript we assessed the roles of those TLRs, cytokines and chemokines in the central nervous system (CNS) of the mouse brain post JEV infection by intracerebral and tail vein route. For this, we developed the mouse model of encephalitis by injecting the GP-78 (JEV a neurovirulent strain) virus through IC and TV route. We noticed the upregulated levels of some specific TLRs, cytokines and chemokines in mouse brain following IC and TV challenge at different days post JEV infection. The increased levels of some specific TLRs, cytokines and chemokines have worst outcome in disease progression and tissue pathology at later stage of infection.

Introduction

Japanese encephalitis (JE) is caused by Japanese encephalitis virus (JEV). JEV is enveloped positive-sense single stranded RNA virus and belongs to the genus flavivirus of the *flaviviridae* family. The virus is transmitted by *Culex* mosquito (Triteriorhynchous). Although effective vaccines are available, JE is endemic in many countries and is the most important viral encephalitis worldwide[50]. The JEV frequently causes severe diseases in humans, including encephalitis and leads to significant mortality and long-term neurological sequelae among survivors[49]. JEV infection and its associated immune pathologies and diseases continue to remain a major challenge to public health. The lack of effective antiviral therapies reinforces the need to understand how the immune response to JEV infection is regulated.

JEV induces neuroinflammation, which has been identified as a significant element in JEV pathogenesis in humans including immune cell infiltration and neuronal degeneration[24]. The presence of proinflammatory cytokines can cause a shift or polarization of resting microglia to adopt their activated states. Microglial activation is routinely divided into two main phenotypes, M1 and M2, albeit that microglia can lie anywhere within the broad spectrum between these states[28]. M1 macrophages are activated by IFN-γ, IL-6, ROS, iNOS and TNF-α in what is referred to as classical activation. Classical activation results in proinflammatory cytokine release, lymphocyte recruitment and a strengthened immune response.

M2 macrophage activation, also referred to as alternative activation, has neurotrophic and anti-inflammatory effects and leads to tissue repair. Alternative activation occurs as a result of stimulation by IL-4/10/13 and TGF-β. The M1:M2 phenotypic ratio is greater in times of injury and higher ratios have been associated with chronic inflammation[2,48]. The innate immune response plays a crucial role in the initial control of JEV infection and causes an inflammatory process[34]. When inflammatory pathways are mis-regulated, an acute inflammation can become chronic and exacerbate disease. There are many studies describing the role of inflammatory mediators (cytokines, chemokines, metalloproteinases and TLRs) in disruption of blood brain barrier and their involvement in disease progression following viral infection in brain.

For instance, elevated CAM expression is reported to occur during infection of mice with multiple neurotrophic viruses such as West Nile virus (WNV), Japanese encephalitis virus (JEV) and Venezuelan equine encephalitis virus (VEEV)[44]. Pharmacological blockade ofVCAM-1 or its ligand ameliorated the severity of immunopathology associated with WNV infection[10]. However, current studies do not describe the innate immune pathways that cause inflammatory responses in microglia infected by JEV.

There are few studies demonstrating the involvement of TLRs in the etiology of JEV infection. However, the exact mechanism is yet to be determined. The involvement of toll-

like receptors (TLRs) in the inflammatory response during the early stages of JEV infection has been studied but is still not fully understood[54]. Earlier studies have demonstrated that TLR2 mediates a parasite-induced inflammatory response[51], although the mechanism underlying the TLR2-mediated inflammatory response in JEV infection has not been elucidated in detail.

In our previous study, we investigated the expression profile of TLRs, cytokines and chemokines in JEV infected microglial cell line BV2 and neuronal cell line Neuro 2A. Our results demonstrated the exaggerated release of some specific TLRs, cytokines and chemokines in *in vitro* cell culture of microglial and neuro 2A cell line, which is associated with bad outcome in *in vivo* study (this study).As there is an urgent need to better understand the role of inflammatory mechanisms following JEV infection in exacerbating the tissue damage, our present study in addition to our previous *in vitro* results[45] provides further understanding of JEV-induced microglial cell inflammation and provides a basis for preventing inflammation-induced neuronal damage in the future.

For better understanding of virus-neuron cell relationship following JEV infection in CNS, it is crucial to investigate the role of TLRs, cytokines and chemokines in CNS. Hence, to study the *in vivo* effect of JEV in CNS, we developed the mouse model of encephalitis to study the role immune mediators in disease progression following JEV infection.

Material and Methods

Mice inoculation, clinical sign /symptoms and Sacrifice schedule: Six to eight week-old female inbred BALB/c mice were procured and housed at animal house, Sanjay Gandhi Post-Graduate Institute of Medical Sciences Lucknow. A total of 60 mice were enrolled into the present study. Mice were randomly distributed in the number of groups. Thirty (30) mice were used for the virus-infected group by tail vein (TV) route and another 30 mice were used for virus-infected group by IC (Intracerebral route). Out of 30 mice for each study group, 15 mice were used for the mock-infected control. The experimental paradigm is given in figure 1.

For intra-cerebral (IC) route infected group: Out of 30 mice, 15 mice were inoculated with JEV (strain GP-78668A) of 3 x 10^6 plaque forming units (PFU) by intra-cerebral route (IC). Sterile phosphate buffered saline (PBS) was inoculated in rest 15 mice (age and sex matched control) and used as mock control group. Mice were monitored daily for sign, symptoms of encephalitis and survival. The mice were euthanized aseptically 0, 1, 3, 5 and 7 day post infection. At each time point, 3 mice each from both control and virus-infected groups were selected. Brain was excised aseptically and stored at -80^{0}C for future study.

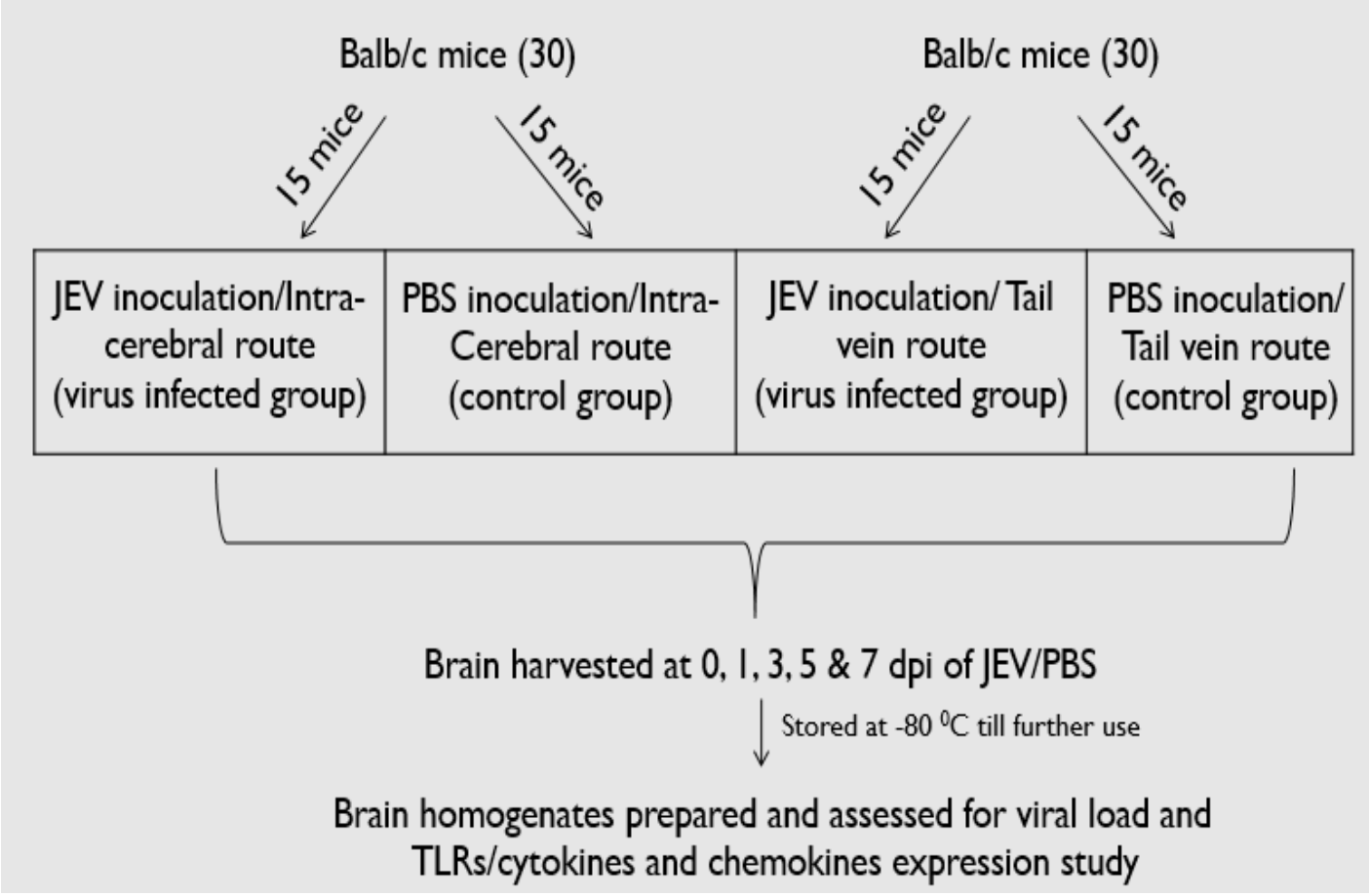

Figure 1: Experimental paradigm. Balb/c mice were inoculated with JEV/PBS and brain were harvested at different days post inoculation for expression profile study of specific TLRs/ cytokines/ chemokines.

For tail vein (TV) route infected group: Out of 30 mice, 15 mice were inoculated with JEV (strain GP-78668A) of 3 x 10^6 plaque forming units (PFU) by tail vein (TV). Sterile phosphate buffered saline (PBS) was inoculated in rest 15 mice (age and sex matched control) and used as mock control group. Mice were monitored daily for sign, symptoms of encephalitis and survival. The mice were euthanized aseptically 0, 1, 3, 5 and 7 day post infection. At each time point, 3 mice each from both control and virus-infected groups were selected. Brain was excised aseptically and stored at -80^{0}C for future study. The virus stocks were titrated by plaque assay and were stored in aliquots at −80°C until use

JEV, {GP78668A (GP-78)} propagation done in BALB/c mice brainand virus titer was determined by standard plaque assay[45]: An Indian non-neuroinvasive but neurovirulent strain of JEV, GP78668A (GP-78) was used throughout the study. The virus was propagated in the brain of suckling mice by intracerebral (IC) injection. Mice were procured and housed at an animal care facility of our Institute i.e. Sanjay Gandhi Post Graduate Institute of Medical Sciences (SGPGIMS), Lucknow, India. Mice were fed with protein rich diet and water *ad libitum*. The animals were maintained in an air conditioned room (25 ± 2 ºC) with 12-h light and dark cycle (7 a.m.–7 p.m.). All the experiments were performed during the light cycle between 10 a.m. and 2 p.m. and were normalized in all mice. The study was approved by the institutional ethics committee and all the experiments were carried out in accordance with the institutional guidelines on the care and use of experimental animals.

A total of 50µl from virus stock was injected for virus propagation. After 4 days of JEV injection, the mice were deeply anesthetized with isoflurane and euthanized in aseptic condition in BSL-2 facility. The mice brains were harvested in aseptic condition and freezed immediately at -70^{O}C and later homogenized in sterile phosphate buffered saline (PBS) and centrifuged at 13,000 rpm for 30 min at 4ºC. The supernatant was collected, aliquoted and stored at -70ºC till further use. The virus titration was done on stable porcine kidney (PS) cell line by plaque assay as per standard procedure.

Plaque Assay: In brief, PS cell monolayer was grown in 6-well tissue culture plates (Nunc, Denmark). Ten-fold serial dilutions of the propagated virus were made with 2 % minimum essential medium (MEM). To the 75–80 % confluent PS cell monolayer, 200 µl of each serial dilution was added and adsorbed by frequent shaking for 1 h at 37 ºC with 5 % CO_2. Only MEM was used as a negative control.

After adsorption, the cell monolayers were washed with PBS to remove the unadsorbed virus particles. To each well, 3 ml overlay media (a mixture of equal volumes of 1 %agarose (kept at 45 ºC) and 2X MEM (kept at 37 ºC) were poured and allowed to solidify at room temperature (RT).

The plates were then incubated for 4 days at 37 ºC with 5 % CO_2. After 4 days of incubation, the cells were fixed by adding 10 % formaldehyde for 2 h at RT. The overlay media were carefully removed with spatula and the cells were stained with 1 % crystal violet. Plaques at different dilutions were counted manually and the dilution showing number of plaques in the range of 20–200 was selected for determination of virus titer using the following formula:

Plaque forming units PFU/ml =1/ dilution X no of plaques X 1/ml of inoculum/well

Body Weight: Body weights of mice from both, the virus infected and control groups were assessed post JEV infection at 0, 1, 3, 5 and 7 days post infection.

Blood brain barrier integrity test performed for mock infected control and JEV infected mice: BBB integrity was evaluated with Evan's blue dye exclusion test. Mice were grouped as control group and JEV infected group. Three mice each from control and JEV infected group (IC injection) at each time points i.e. 1, 3, 5 and 6 dpi were injected intravenously with 75µl of 2% Evan's blue (Sigma) in PBS. One hour later, mice were sacrificed and transcardially perfused with 10 ml of normal saline. Brains were then removed and photographed.

Histology and Immunohistochemistry (IHC) experiments carried out to check tissue damage and inflammatory cells migration at the site of infection/damage: Histopathology and IHC of brain tissues were carried out in the Department of Pathology, SGPGIMS, Lucknow, India. The mice were anaesthetized with ether and perfused with 150 ml PBS (0.1 M, pH 7.2). The brain were sliced and fixed in 10% buffered formalin for 3 days. After fixation the tissues were sectioned in 3-5 mm slices and processed overnight. Next day, the tissues were embedded in paraffin blocks. Five micron section were cut and dewaxed in xylene and graded alcohol (absolute 90%, 70%) and brought to water. One section from each block was cut and stained with hematoxylin-eosin (HE). Histopathological evaluation was done by the pathologist. The pathologist who was evaluating the sections was blinded for the treatment group.

For IHC, the sections were cut and lifted on polylysine coated slides and brought to water as above. Antigen retrievel was done in citrate buffer for half an hour at 98^{0}C and at pH 6.0. Endogenous blocking was done by 3% H_2O_2 and was washed in between with TRIS buffered saline. Primary antibody (clone NS1 for JEV protein detection at 1:25 dilution from abcam, USA) was applied for 2 hours at room temperature and washed with Tris buffered saline. Then, secondary antibody (Universal Envision, DAKO) was applied for 30 min and washed with Tris buffered saline and then treated with chromogen (Diaminobenzidine). The slides were counterstained with hematoxylin and mounted with DPX.

Microglia activation investigated following JEV infection in mice brain: To investigate microglial activation in mice brain of JEV infected and control group, mRNA levels of ionized calcium-binding adapter molecule-1 (Iba-1, a specific microglial marker) were measured. Activated microglia contributes to the production of inflammatory cytokines that mediate direct or indirect neuron death.

Ethics statement: All animal experiments were carried out in accordance with the guidelines provided by the institutional animal ethics committee.

Primers used for PCR amplification of target genes: For quantitative Real time PCR (qRT-PCR), oligonucleotide primers for each specific TLRs, cytokine and chemokines were designed using free online primer design tool (http://bioinfo.ut.ee/primer3-0.4.0/primer3/) i.e. "Primer3 Input (version 0.4.0)". The selected primers were subjected to an extensive search using BLAST tool (www.ncbi.nlm.nih.gov/blast) for species specificity.

Quantitative real-time RT-PCR for viral burden and cytokines, chemokines and tlrs expression in mock infected control and JEV infected mice from both the group i.e. IC route inoculation and TV inoculation: RNA was extracted using the QIAamp Viral RNA Mini Kit (QIAGEN) from brain homogenates prepared from mock infected control mice brain and JEV infected mice brain (from both the group i.e. IC route inoculation and TV inoculation) according to the manufacturer's instructions. To detect and quantify the JEV RNAs, commercially available kit (Genome diagnostic) was used according to the manufacturer's instruction. Primers were specific for a 130 bp region of the JEV envelop gene. The probe was labeled with the reporter dye FAM at the 50 end and the quencher dye TAMRA at the 30 end. The reaction condition was 50^0C for 15 min, 95^0C for 10 min,45 cycles of 94^0C for 10 s, 55^0C for 20 s and 72^0C for15 s, using the ABI 7500 Real Time PCR System (Applied Bio systems, Foster City, CA, USA). Water (PCR grade) was used as a negative control.

The TLRs, cytokines and chemokines levels in mock infected control mice brain and JEV infected mice brain (from both the group i.e. IC route inoculation and TV inoculation) were quantified using quantitative TaqMan - based real-time qRT-PCR. Total RNAs from brain homogenates were extracted as per manufacturer's instructions. RNA was quantified by measuring the optical density at 260 nm (OD_{260}) using a Nanodrop-1000 spectrophotometer (Thermo Scientific) and the purity was assessed by determining the OD_{260}/OD_{280} ratio, which was between 1.9 and 2. One µg of extracted RNA was then used in real-time qRT-PCR. Following reverse transcription of total RNAs using a High-Capacity cDNA Reverse Transcription Kit (Applied Biosystems, Foster City, CA, USA), a reaction mixture containing 1 µl of template cDNA, 10 µl of 2× Premix x Taq and 600 nM primers in a final volume of 20 µl was prepared. No template control (NTC) reactions were performed along with the PCR to identify PCR contamination.

Table 1
Primers sequences for expression study of TLRs, Cytokines and Chemokines

Gene Name	Primer Sequence (5'-3')	Location	Gene Bank ID
TLR-2	F-GCAAACGCTGTTCTGCTCAG	56-75	NM_011905
	R-AGGCGTCTCCCTCTATTGTATT	286-265	
TLR-4	F-AGGCACATGCTCTAGCACTAA	287-307	NM_021297
	R-AGGCTCCCCAGTTTAACTCTG	368-348	
TLR-9	F-ATGGTTCTCCGTCGAAGGACT	1-21	NM_031178
	R-GAGGCTTCAGCTCACAGGG	118-100	
IFN-γ	F-ATGAACGCTACACACTGCATC	1-21	NM_008337
	R-CCATCCTTTTGCCAGTTCCTC	182-162	
IL-6	F-CCAAGAGGTGAGTGCTTCCC	462-481	NM_031168
	R-CTGTTGTTCAGACTCTCTCCCT	579-558	
IL-17	F-TCT GAT GCT GTT GCT GCT G	87–105	NM_010552.3
	R-ACG GTT AGA GGT AGT CTG AGG	254–267	
IL-21	F-GGACCCTTGTCTGTCTGGTAG	8-28	NM_021782
	R-TGTGGAGCTGATAGAAGTTCAGG	173-151	
Foxp3+ regulatory T cells	F- GGC CCT TCT CCA GGA CAG A	551–570	NM_054039.2
	R-GCT GAT CAT GGC TGG GTT GT	642–662	
RANTES(CCL-5)	F-GCTGCTTTGCCTACCTCTCC	98-117	NM_013653
	R-TCGAGTGACAAACACGACTGC	201-181	
MCP-1(CCL-2)	F-TTAAAAACCTGGATCGGAACCAA	260-282	NM_01133 3
	R-GCATTAGCTTCAGATTTACGGGT	380-358	
β-actin	F-TGG AAT CCT GTG GCA TCC ATG AAA C	885–909	NM_007393.3
	R-TAA AAC GCA GCT CAG TAA CAG TCC G	1209–1233	

The conditions used for qRT-PCR are as follows: 95°C for 2 min (hold), 94°C for 15 s, 60°C for 15 s and 72°C for 1 min (40 cycles). All samples were run in triplicate. The dissociation curves were generated to check for the specificity of primer annealing to the template. The levels of cytokines, chemokines and TLRs mRNAs were normalized to the levels of the rat housekeeping gene β-actin of the same sample. Relative changes of gene expression were calculated by the $2^{-\Delta\Delta Ct}$ formula and the data are represented as percentage change of the control group.

Statistical analysis: All of the statistical analyses were done using PRISM software. Student's t test for independent groups was performed to compare the cytokines, chemokines and TLRs levels between mock-infected control and virus-infected mice. Differences in expression with the time course were analyzed by One-way analysis of variance (ANOVA) using Tukey's test with multiple post hoc analyses. $p<0.05$ was considered statistically significant.

Results

Mice survival, clinical signs and symptoms: All the mice in the mock infected controls were healthy with no clinical sign and symptoms at any time point. In the virus infected mice, 100% mortality was observed after 7 dpi. Thus, we have chosen time point up to 6dpi in our study group. In the virus infected group, hunching of the back and slight hind limb disability was observed on 4 dpi. The typical symptoms of encephalitis characterized by total hind limb paralysis, tremors and convulsions with altered consciousness became evident on 5 dpi and 6 dpi (Fig. 2A, B, C). Mice were almost moribund when they were sacrificed. The mice brain were harvested in aseptic condition at BSL-3 facility of SGPGIMS, Lucknow and stored at -80°C until further use.

Body Weight: Drop in body weight of JEV-infected mice was noticed at each time point compared to mock control (Fig. 2D).

Virus growth assay: To study the virus multiplication in the brain of virus infected mice, at each time points of sacrifice, the virus titer was determined by plaque assay. A significant increase from 9.9×10^6 PFU/g at 3 dpi to 1.3×10^8 PFU/g at 5 dpi was noted. This increased further to 2.0×10^9 PFU/g in the brain of virus infected mice at 6 dpi (Fig. 2E).

JEV infection via tail vein damages the blood brain barrier (BBB) in mice: Evan's blue is a cationic dye that binds to serum albumin to form a dye- protein complex that cannot pass through the intact BBB. Due to this, it is used as a standard molecule to test the permeability of the BBB. Intravenous injection of Evan's blue results in the formation of a conjugate with serum albumin. Inclusion of the blue colored dye in the brain indicated the passage of the dye protein conjugate into the brain that signifies increased permeability or damage of BBB. Mice from control group and JEV infected group was taken to test the BBB permeability (Fig. 2F). Compared to mock-infected control, the leakage of Evan's blue dye in the JEV infected mice brain started at 3dpi which was more prominent at 6 dpi. This clearly indicates the compromised BBB integrity in virus infected mice brain with respect to control.

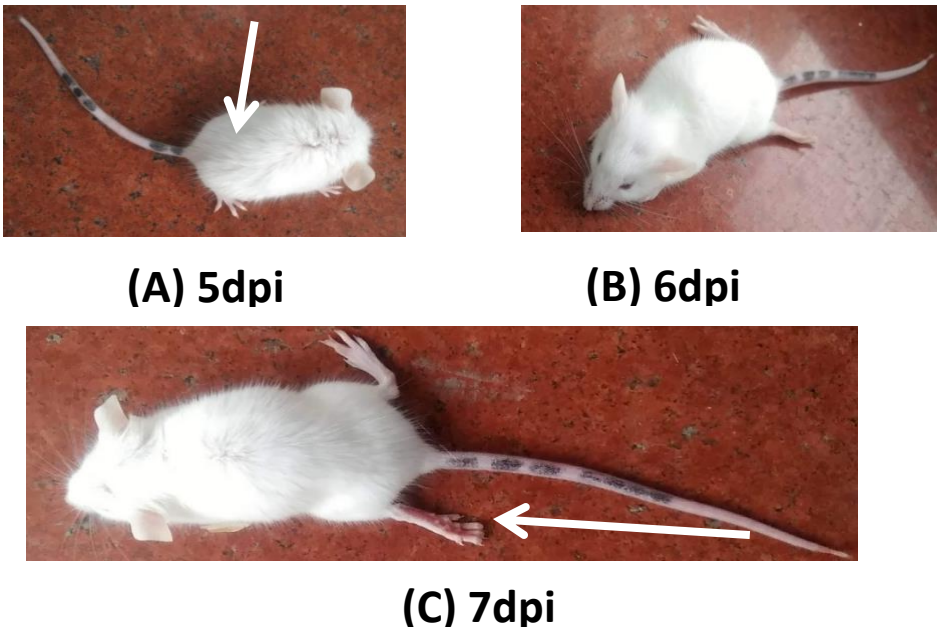

Figure 2 (A, B, C): Virus propagation in mice brain: Mice were inoculated intracerebral (IC) with GP-78 strain of Japanese encephalitis virus
(A) Hunching of the back (indicated by arrow) and slight hind limb disability was observed on 5 dpi.
(B and C) The typical symptoms of encephalitis characterized by total hind limb paralysis (indicated by arrow), tremors and convulsions with altered consciousness became evident on 6 and 7 dpi. The mice were almost moribund when they were sacrificed

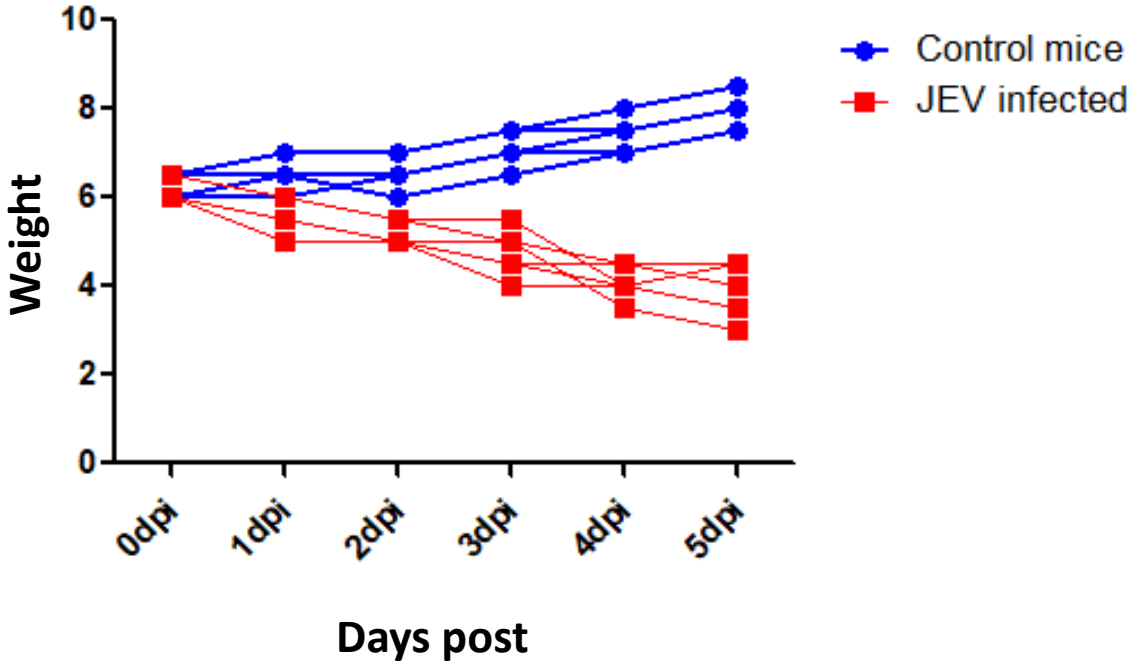

Figure 2D: Balb/c mice were infected with JEV. PBS inoculated mice were used as mock control. Body weight of mice from both the groups were measured at different day post infection. The drop in body weight of JEV-infected mice was noticed compared to mock controls.

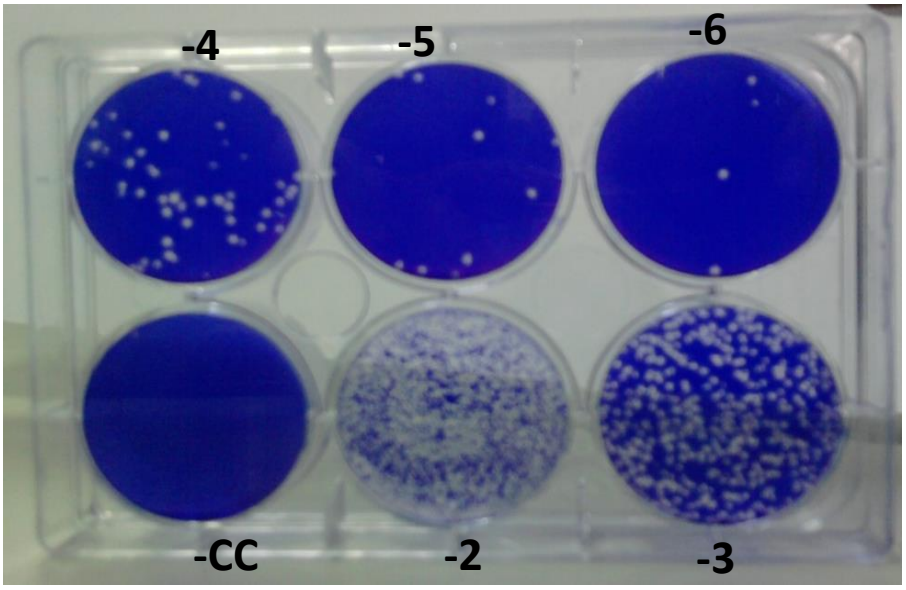

Figure 2E: six well tissue culture plates demonstrating the virus titration from the brain of intracerebrally inoculated mice.

Neuropathological changes: Section from mouse brain stained with HE showed neuronal damage in the form of neuronal shrinkage and hypereosinophilia. There was edema, spongy degeneration and infiltration by neutrophil and lymphocytes within the brain parenchyma around neurons more in the thalamic and hypothalamic area followed by cerebral cortex. Perivascular inflammatory infiltrate was seen. Cerebellum showed only mild neuronal damage displaying shrinkage and hypereosinophilia (Fig 3a-h). These changes in the brain parenchyma were appreciable at 5th dpi and were more intense on 6th dpi.

Immunohistochemistry (IHC): IHC was performed to look for the presence JEV. Our IHC results showed JEV infected neurons in the hypothalamus, thalamus and cortex. Cerebellum neurons did not show presence of JEV NS1 antigen. The antigen was first visible at 5th day post infection and more pronounced on the 6th day post infection (Fig. 4a-f).

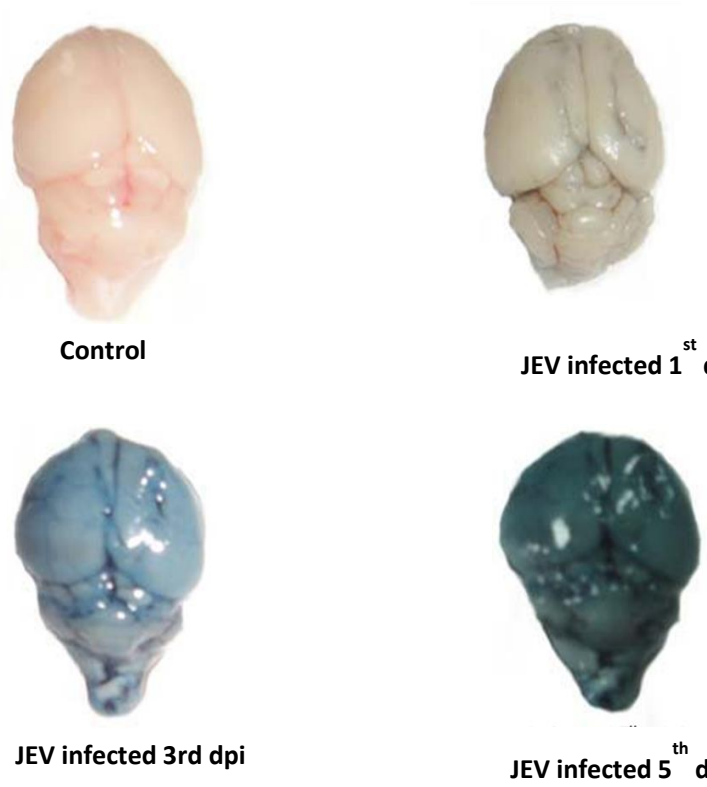

Figure 2F: Blood brain barrier damage of mice infected with JEV (IC challenge) by Evan's blue dye exclusion test.

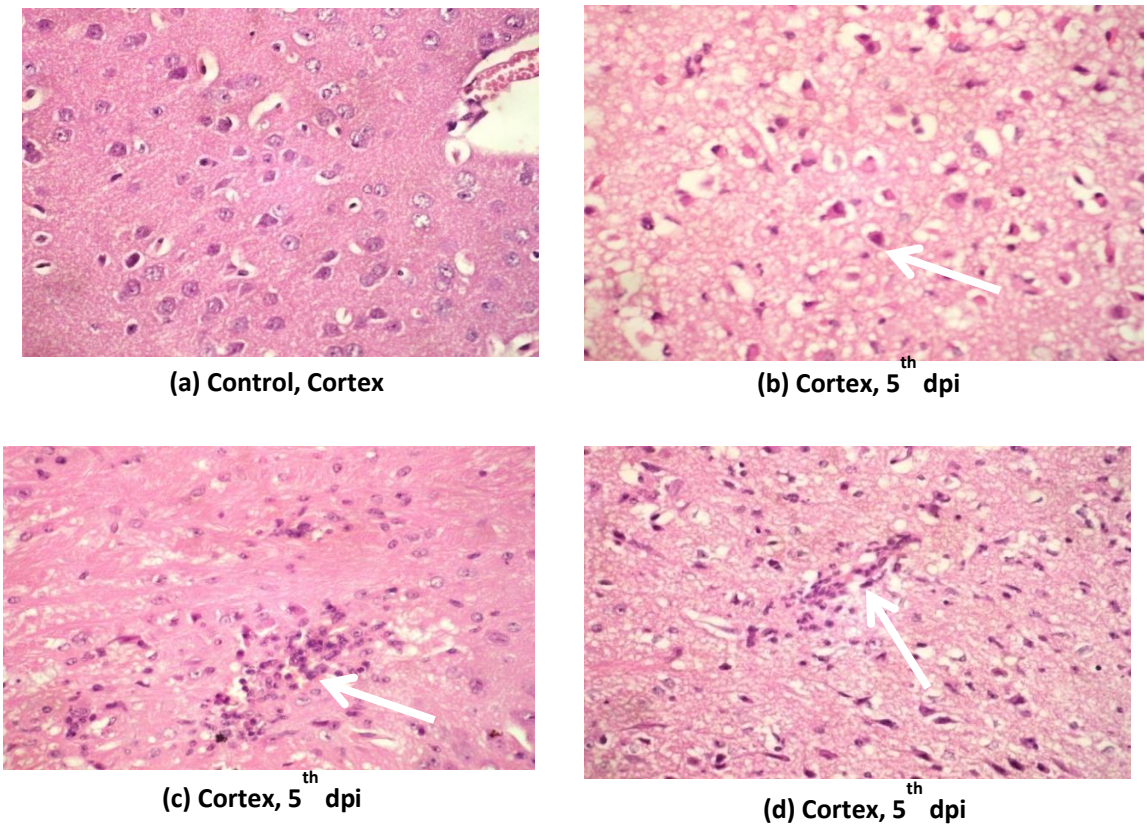

Figure 3: Photomicrograph of H and E staining showing (a) normal appearing neurons with round nuclei, vascular chromatin, prominent nuclei and moderate cytoplasm in cortex of control mice brain, (b) neuronal shrinkage with shrunken nuclei and hypereosinophilic cytoplasm, (c) inflammatory cell infiltrate with in the brain parenchyma causing neuronal damage, (d) perivascular inflammatory cells and neuronal damage at 5th dpi (Magnification at X40)

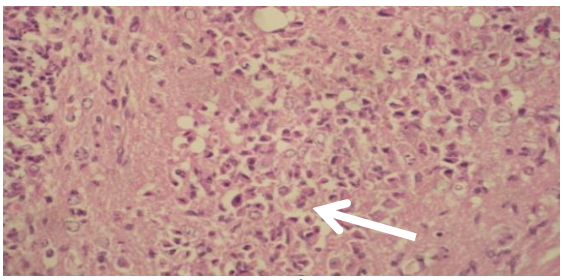

(e) Cortex, 6th dpi

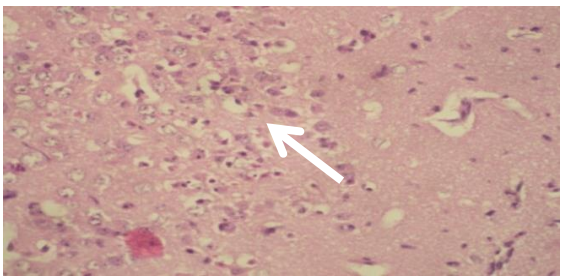

(f) Hypothalamus, 6th

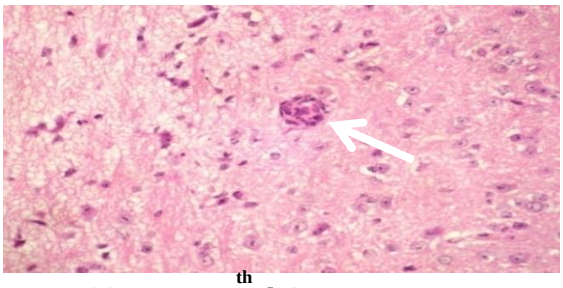

(g) Cortex, 6th dpi

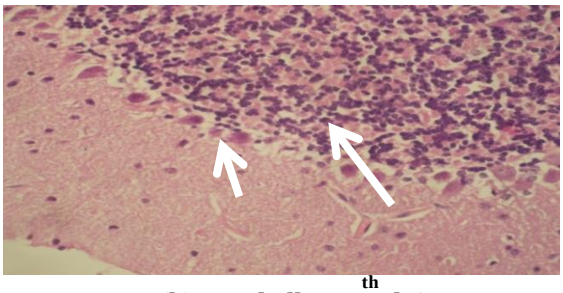

(h) Cerebellum,6th dpi

Figure 3: (e) intense inflammatory infiltration causing necrosis of brain parenchyma, (f) inflammatory infiltrate and neuronal damage, (g) perivascular inflammation in the cortex, (h) Cerebellum showing neuronal shrinkage and hypereosinophilia of the purkinjee cells at 6th dpi (Magnification at X40).

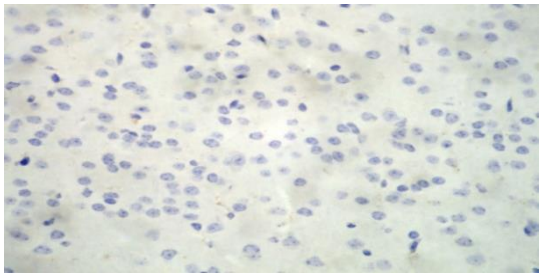

(a) Control, Cortex

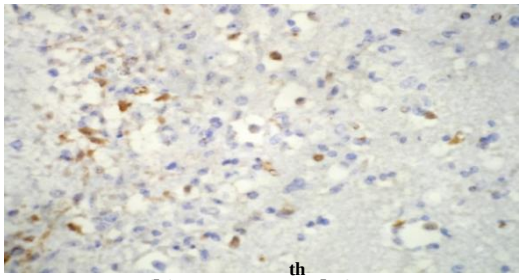

(b) Cortex,5th dpi

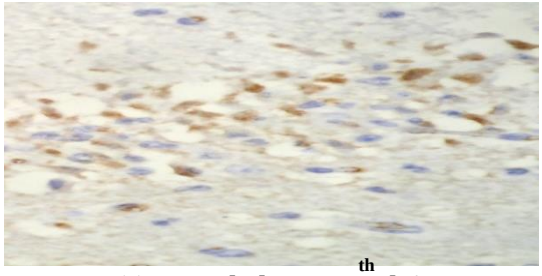

(c) Hypothalamus, 5th dpi

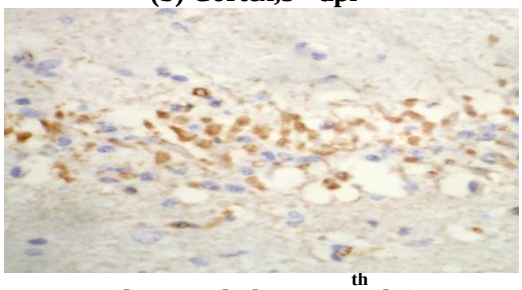

(d) Hypothalamus, 6th dpi

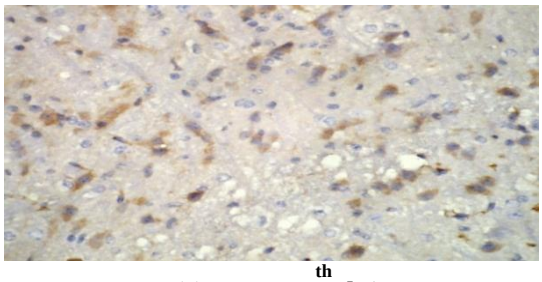

(e) Cortex,6th dpi

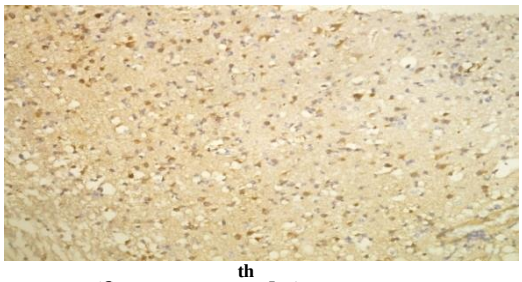

(f) Cortex, 6th dpi, X20

Figure 4: Photomicrograph showing presence of JEV antigen in cortex and hypothalamus region of BALB/c mouse brain infected with $3X10^6$ pfu /ml of JEV(GP-78) at 5th and 6th dpi.

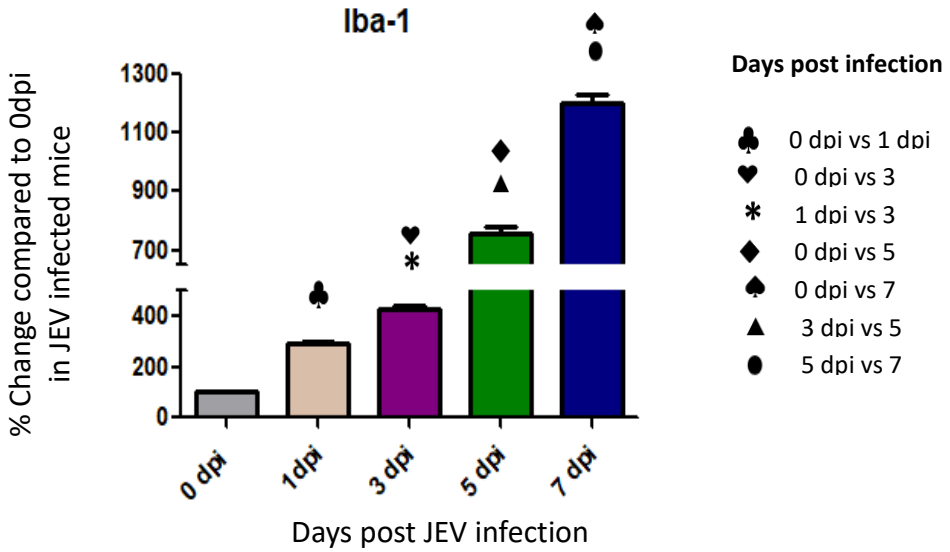

Figure 5: Expression of Iba-1 in JEV infected mice at different (0,1,3,5 and 7 dpi) dpi. Balb/c mice were infected with JEV. mRNA expression was analyzed at different dpi by qPCR. Bar Graph represents the quantification of Iba-1 normalized to β-actin. Values are means± SD of 3 animals at each dpi.

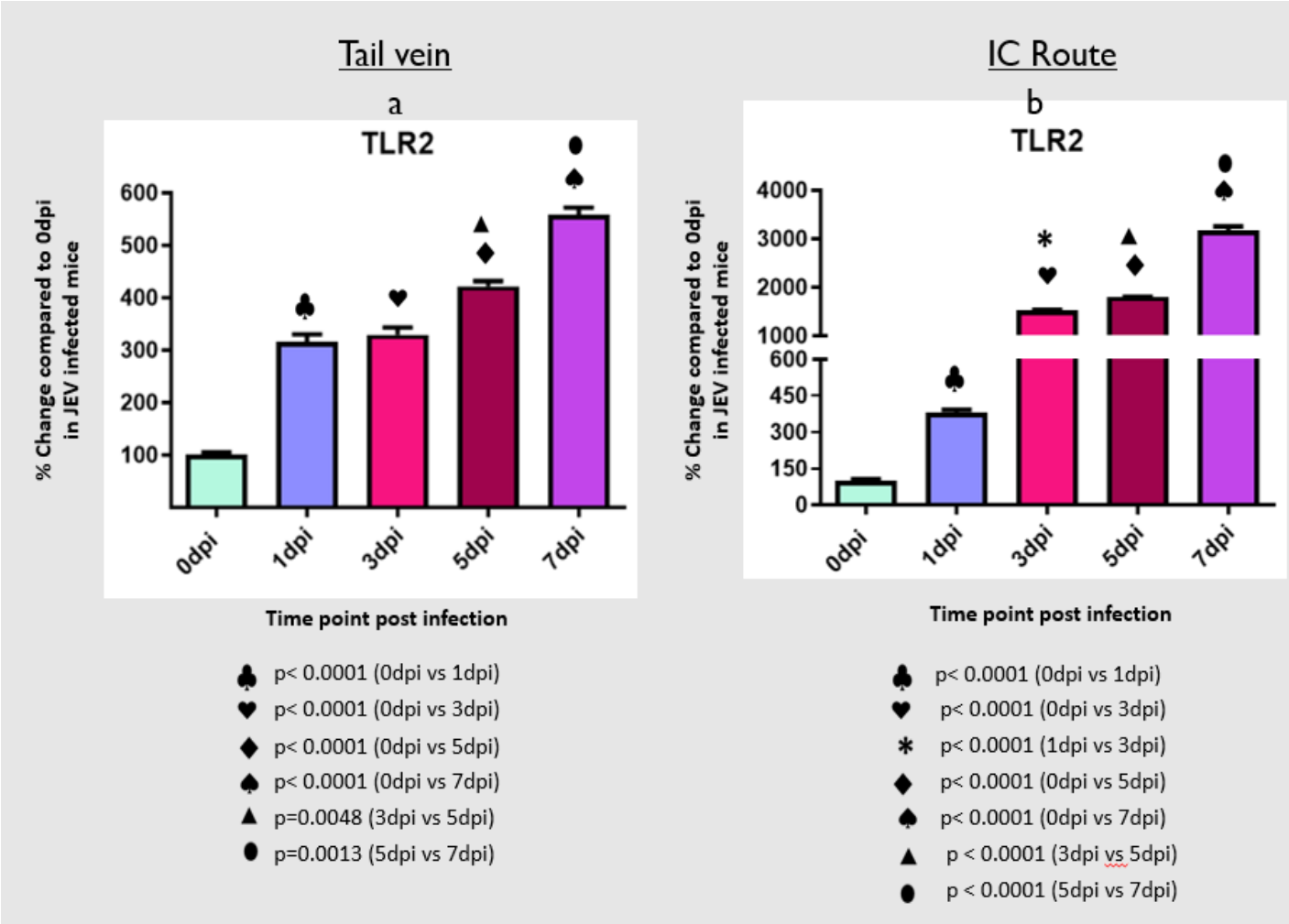

Figure 6: Expression of TLR 2 in Japanese encephalitis virus (JEV) infected mice (a) TV route and (b) IC route, at different (0,1,3,5 and 7 dpi) dpi. Balb/c mice were infected with JEV. mRNA expression was analyzed by qPCR. Bar Graph represents the quantification of TLR2 normalized to β-actin. Data represent mean ± SEM from three independent experiments.

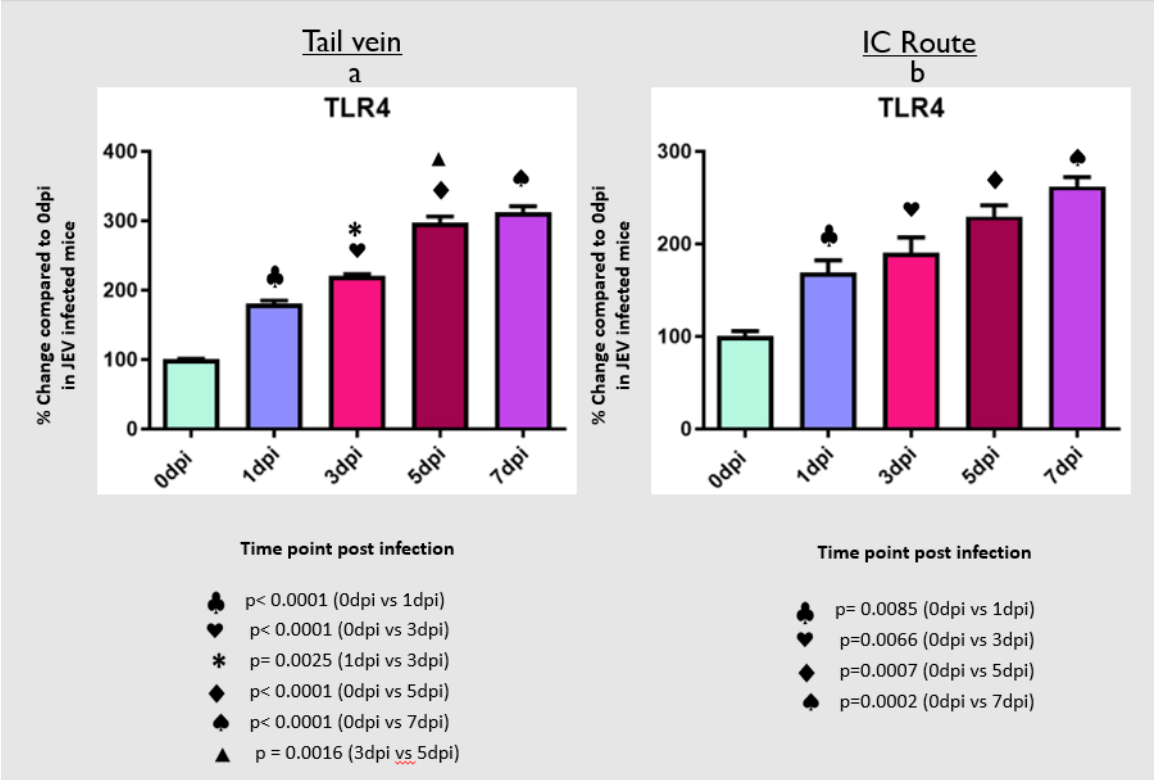

Figure 7: Expression of TLR 4 in Japanese encephalitis virus (JEV) infected mice (a) TV route and (b) IC route, at different (0,1,3,5 and 7 dpi) dpi. Balb/c mice were infected with JEV. mRNA expression was analyzed by qPCR. Bar Graph represents the quantification of TLR4 normalized to β-actin. Data represent mean ± SEM from three independent experiments.

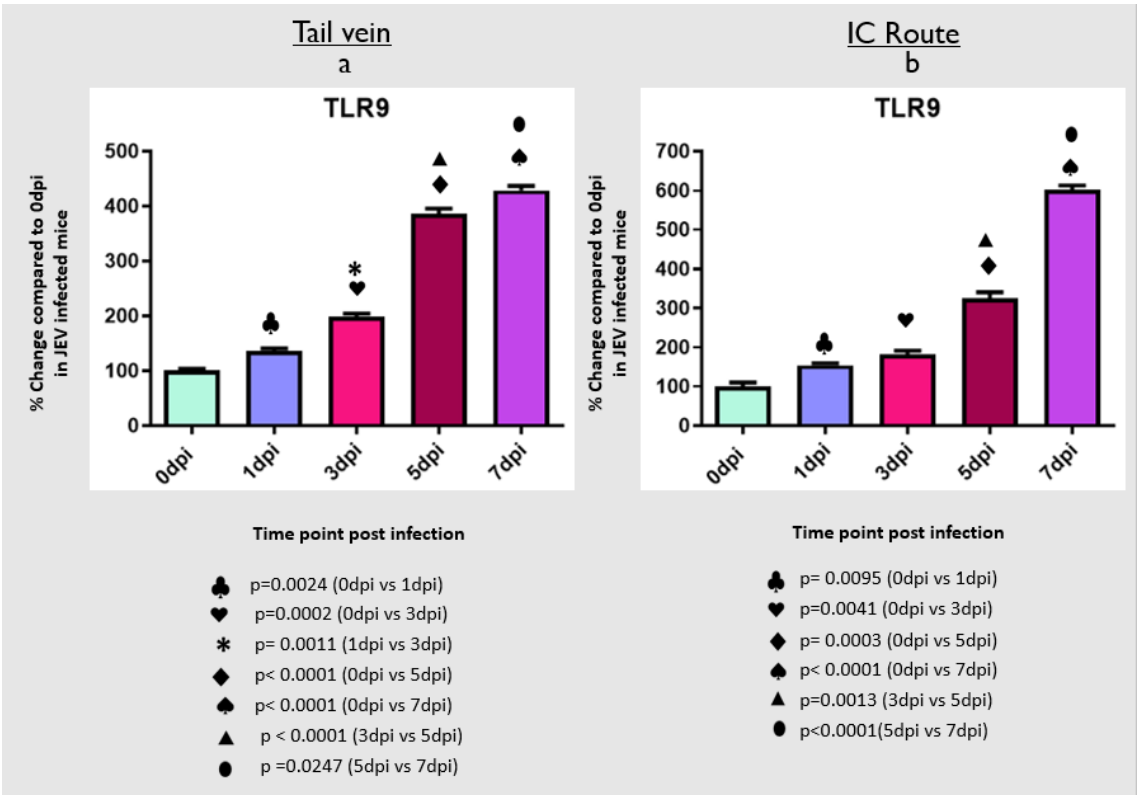

Figure 8: Expression of TLR 9 in Japanese encephalitis virus (JEV) infected mice (a) TV route and (b) IC route, at different (0,1,3,5 and 7 dpi) dpi. Balb/c mice were infected with JEV. mRNA expression was analyzed by qPCR. Bar Graph represents the quantification of TLR9 normalized to β-actin. Data represent mean ± SEM from three independent experiments.

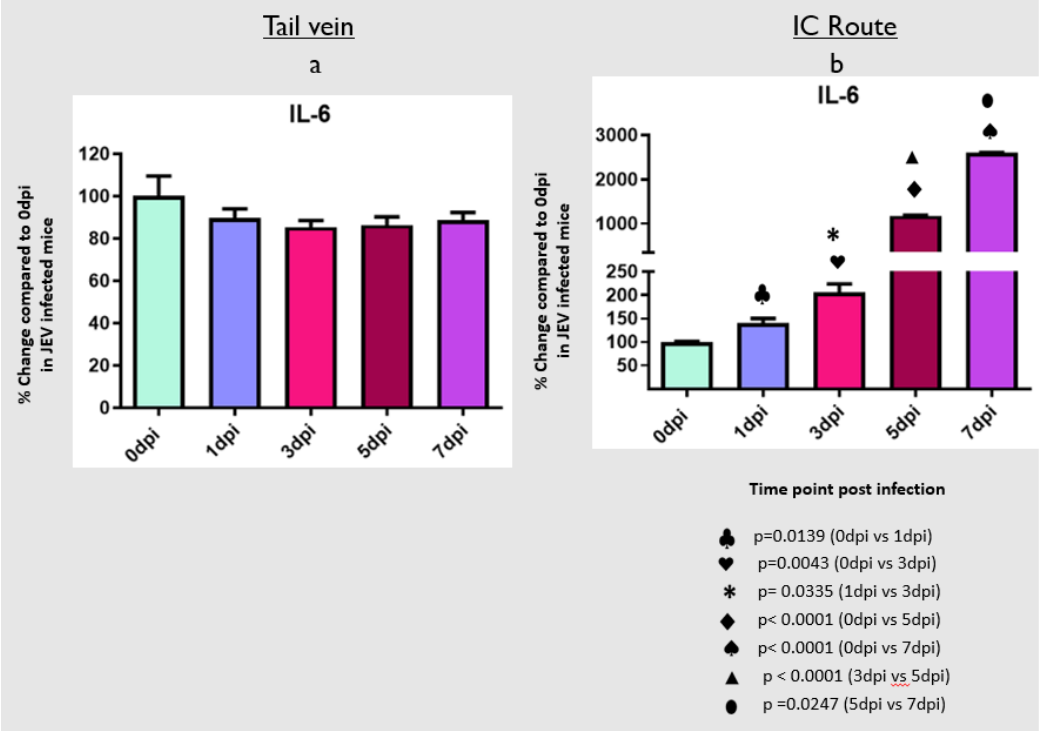

Figure 9: Expression of IL6 in Japanese encephalitis virus (JEV) infected mice (a) TV route and (b) IC route, at different (0,1,3,5 and 7 dpi) dpi. Balb/c mice were infected with JEV. mRNA expression was analyzed by qPCR. Bar Graph represents the quantification of IL6 normalized to β-actin. Data represent mean ± SEM from three independent experiments.

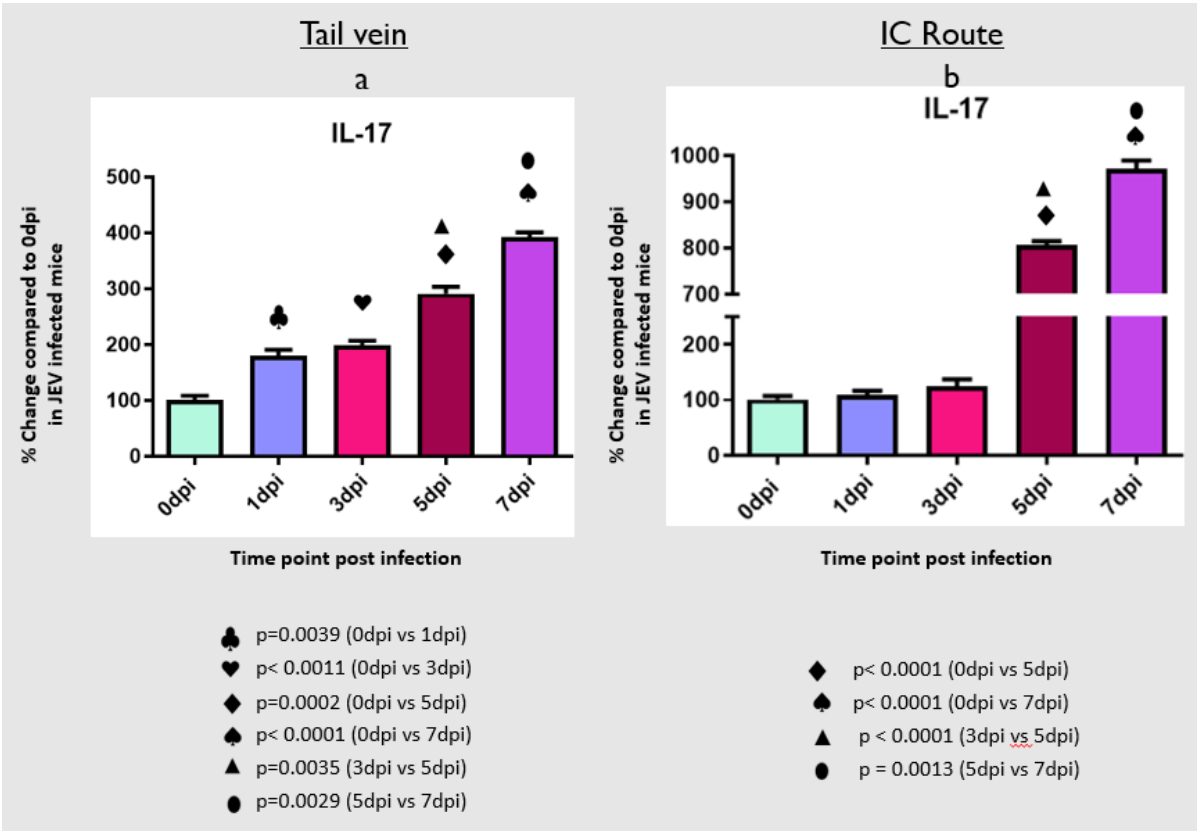

Figure 10: Expression of IL17 in Japanese encephalitis virus (JEV) infected mice (a) TV route and (b) IC route, at different (0,1,3,5 and 7 dpi) dpi. Balb/c mice were infected with JEV. mRNA expression was analyzed by qPCR. Bar Graph represents the quantification of IL17 normalized to β-actin. Data represent mean ± SEM from three independent experiments.

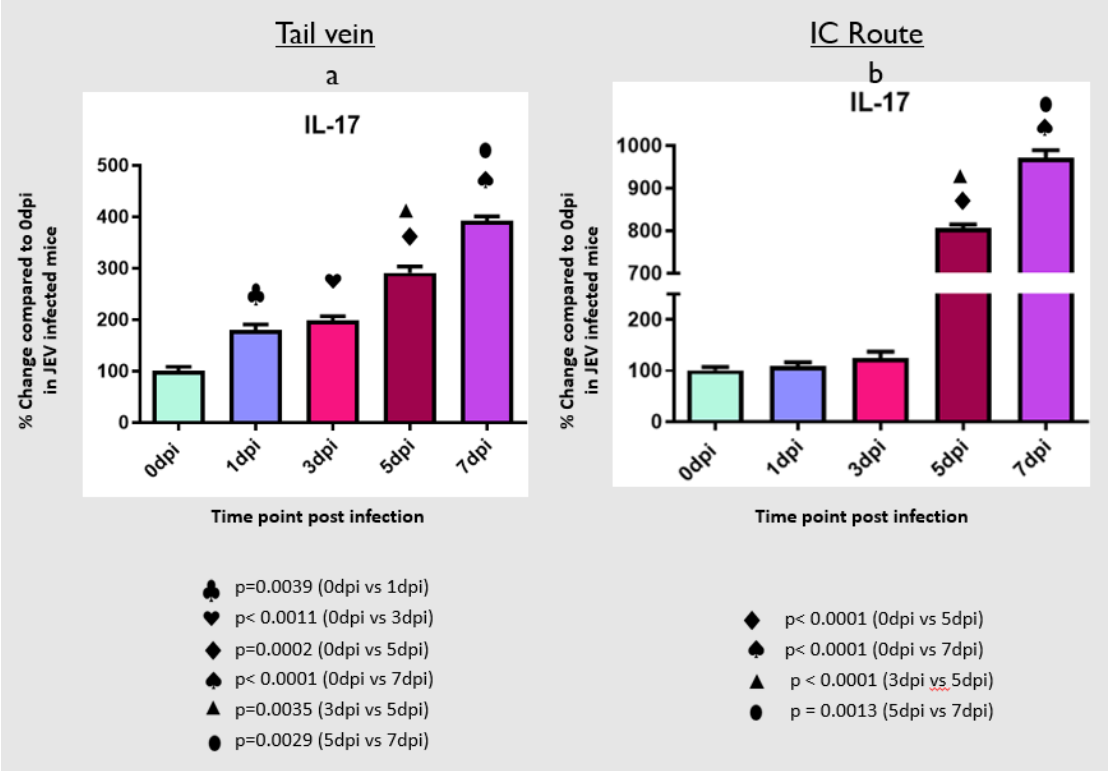

Figure 11: Expression of IL21 in Japanese encephalitis virus (JEV) infected mice (a) TV route and (b) IC route, at different (0,1,3,5 and 7 dpi) dpi. Balb/c mice were infected with JEV. mRNA expression was analyzed by qPCR. Bar Graph represents the quantification of IL21 normalized to β-actin. Data represent mean ± SEM from three independent experiments.

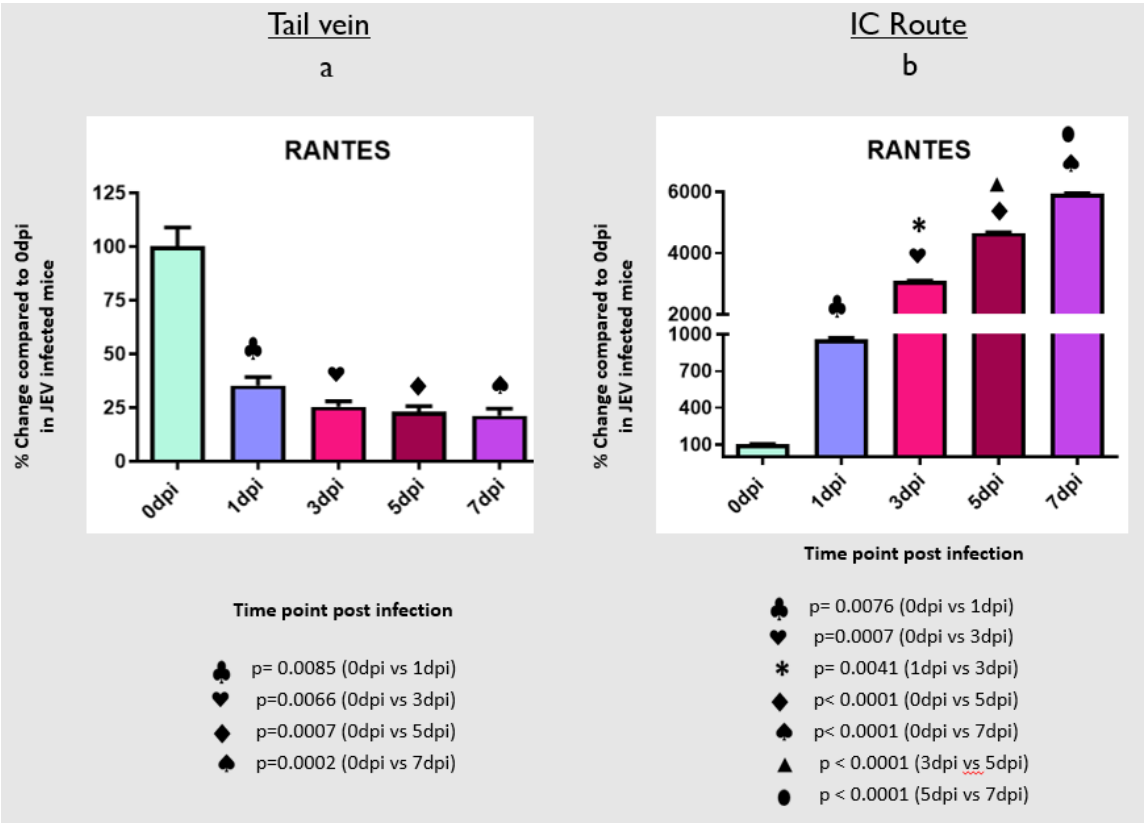

Figure 12: Expression of MCP1 in Japanese encephalitis virus (JEV) infected mice (a) TV route and (b) IC route, at different (0,1,3,5 and 7 dpi) dpi. Balb/c mice were infected with JEV. mRNA expression was analyzed by qPCR. Bar Graph represents the quantification of MCP1 normalized to β-actin. Data represent mean ± SEM from three independent experiments.

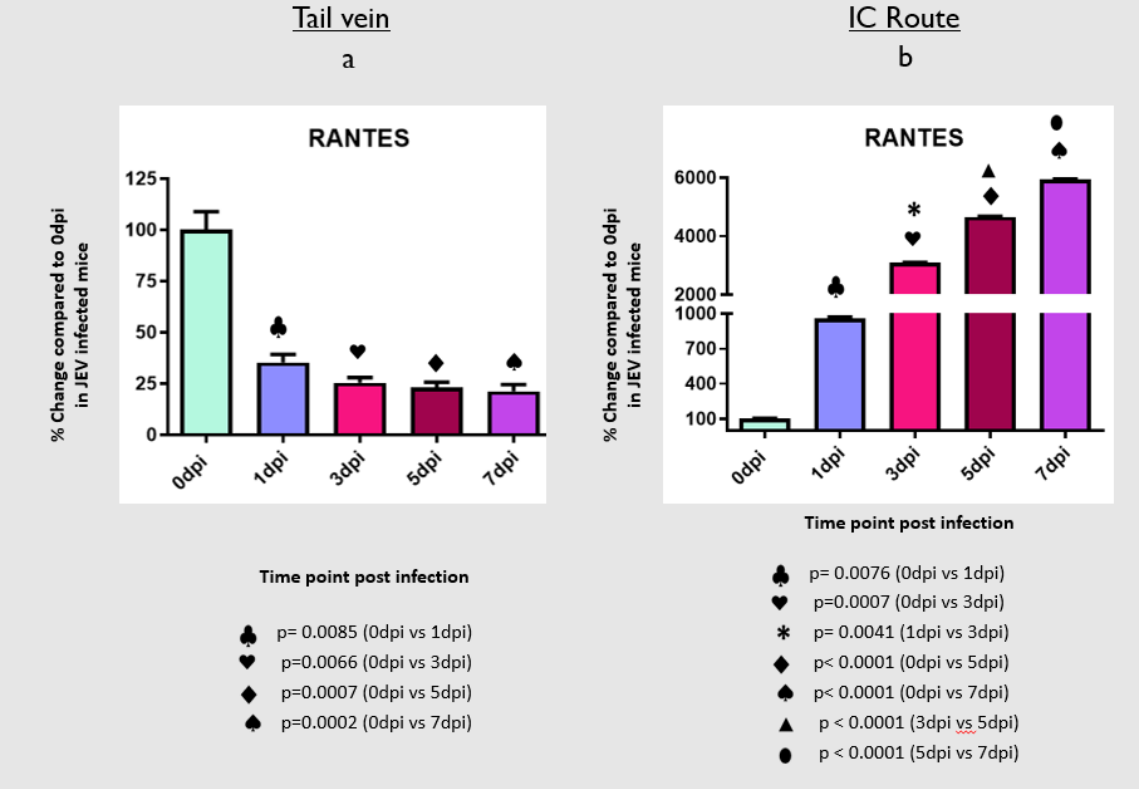

Figure 13: Expression of RANTES in Japanese encephalitis virus (JEV) infected mice (a) TV route and (b) IC route, at different (0,1,3,5 and 7 dpi) dpi. Balb/c mice were infected with JEV. mRNA expression was analyzed by qPCR. Bar Graph represents the quantification of RANTES normalized to β-actin. Data represent mean ± SEM from three independent experiments.

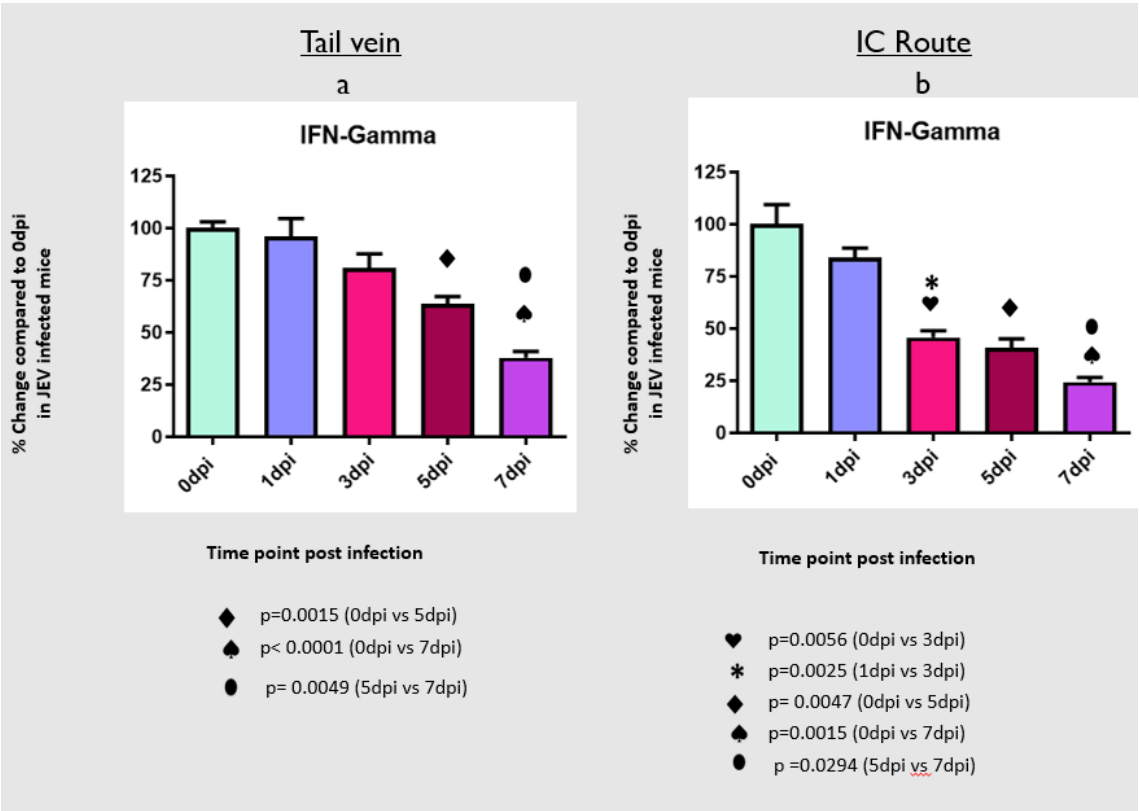

Figure 14: Expression of IFN-ϒ in Japanese encephalitis virus (JEV) infected mice (a) TV route and (b) IC route, at different (0,1,3,5 and 7 dpi) dpi. Balb/c mice were infected with JEV. mRNA expression was analyzed by qPCR. Bar Graph represents the quantification of IFN-ϒ normalized to β-actin. Data represent mean ± SEM from three independent experiments.

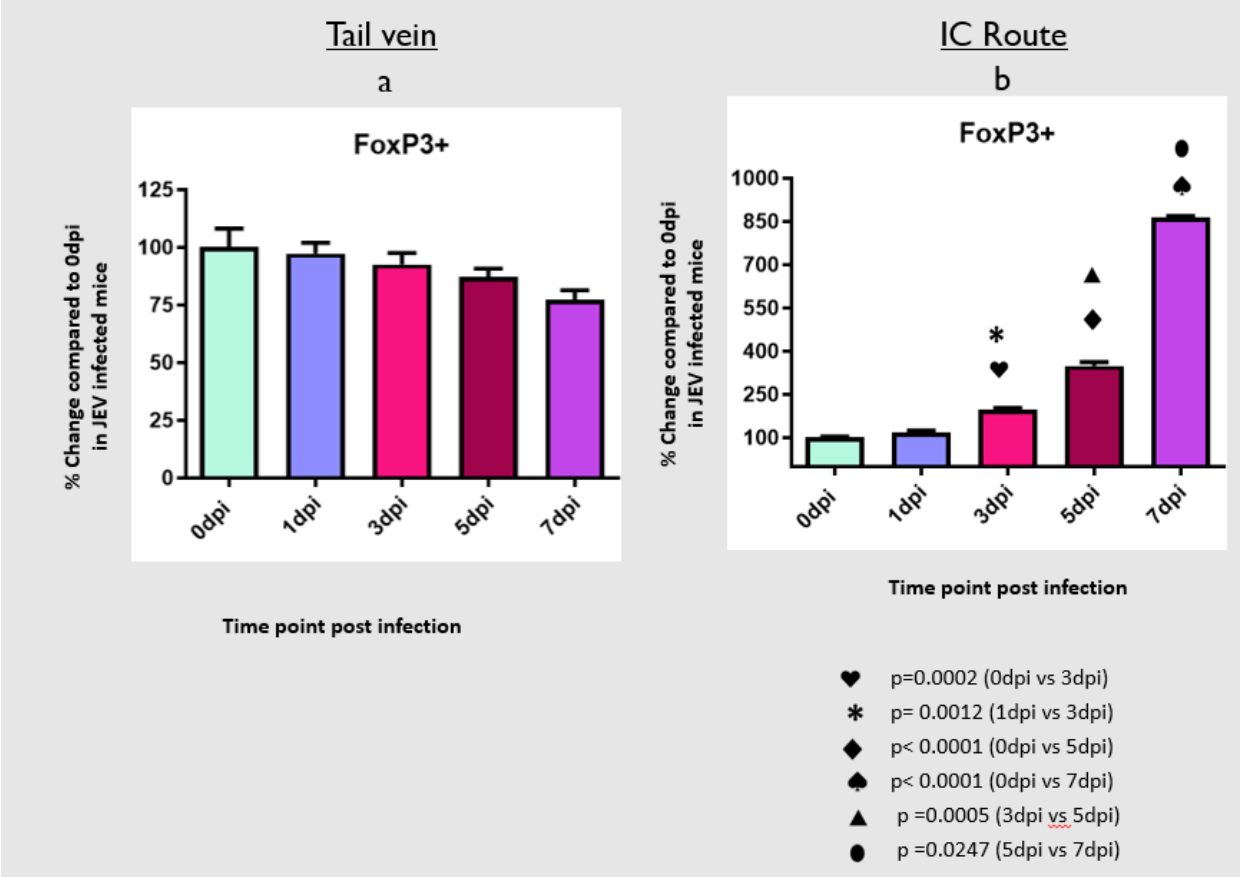

Figure 15: Expression of Foxp3+ in Japanese encephalitis virus (JEV) infected mice (a) TV route and (b) IC route, at different (0,1,3,5 and 7 dpi) dpi. Balb/c mice were infected with JEV. mRNA expression was analyzed by qPCR. Bar Graph represents the quantification of Foxp3+ normalized to β-actin. Data represent mean ± SEM from three independent experiments.

Upregulated microglia activation was noticed in JEV infected mice brain when compared to mock infected controls (Fig. 5). The result clearly indicates that JEV infection induces inflammation in the brain by activation of microglial cells. Activation of microglial cells might play a significant role in inducing neuronal cell death by stimulating the production of proinflammatory mediators. Several authors reported that the levels of various proinflammatory mediators, such as IL-6, IL-1β, TNF-α and MCP-1 were significantly elevated in microglial cells following JEV infection.

Expression levels of TLRs (TLR-2, TLR-4, TLR-9), interleukins (IL-6, IL-17, IL-21), chemokines (MCP-1, RANTES), IFN-ϒ and FOXP3+ in mice brain following compromised of BBB after JEV inoculation via tail vein
Upregulated expression of TLRs (TLR-2, TLR-4, TLR-9) noticed in mice brain following compromised of BBB after JEV inoculation via tail vein
TLR2: The level of TLR2 significantly increased with increasing time points post infection when compared to 0 day post infection (dpi). At 1 day post infection (dpi), the TLR2 level was increased to 316% ($p<0.0001$) which increased significantly at 3dpi (329%, $p<0.0001$), 5dpi (423%, $p<0.0001$) and reached to the level 558% ($p<0.0001$) at 7dpi post infection (Fig. 6a) when compared to the level expressed at 0 day (the value was normalized to 100%) post JEV infection. When we compared the levels expressed between days we noticed a significant 128%, $p=0.0048$ increase in TLR 2 level at 5dpi compared to 3day post JEV infection. At 7dpi the level was significantly increased by 132%, $p=0.0013$ was compared to 5day post infection. Overall we noticed an increase in TLR2 level in mice brain post JEV infection via tail vein at later days of infection compared to 0 dpi. Hence, the TLR2 level was increased with disease progression at later stage of infection (Fig. 6a).

TLR4: The level of TLR4 significantly increased with increasing time points post infection when compared to 0 day post infection (dpi). At 1dpi, the TLR4 level was increased to 180% ($p<0.0001$) which increased significantly at 3 dpi (220%, $p<0.0001$), 5 dpi (297%, $p<0.0001$) and reached to the level 312% ($p<0.0001$) at 7dpi (Fig. 7a) when compared to the level expressed at 0 day (the value was normalized to 100%) post JEV infection. When we compared the levels expressed between day we noticed that TLR 4 level increased to 122% at 3dpi compared to 1day post JEV infection and this increase was significant ($p= 0.0025$). The135%, $p = 0.0016$ increase at 5dpi was noticed compared to 3 day post infection. At 7dpi, the level was increased slightly compared to 5day post infection. But those increases in TLR 4 levels were not significant. Overall we

noticed an increase in TLR4 level in mice brain post JEV infection via tail vein at later days of infection compared to 0dpi. Hence, the TLR4 level was increased with disease progression at later stage of infection (Fig. 7a).

TLR9: The level of TLR9 significantly increased with increasing time points post infection when compared to 0 day post infection (dpi). At 1dpi, the TLR9 level was increased to 137% (p=0.0024) which increased significantly at 3dpi (199%, p=0.0002), 5dpi (386%, p<0.0001) and reached to the level 429% (p<0.0001) at 7dpi (Fig. 8a) when compared to the level expressed at 0 day (the value was normalized to 100%) post JEV infection. When we compared the levels expressed between days, we noticed a significant 196% (p<0.0001) increase in TLR9 levels at 5dpi compared to 3 day post infection. At 7dpi the level was significantly increased by 111%, p =0.0247 was compared to 5day post infection. Overall we noticed an increase in TLR9 level in mice brain post JEV infection via tail vein at later days of infection compared to 0 dpi. Hence, the TLR9 level was increased with disease progression at later stage of infection (Fig. 8a).

Down-regulated expression of interleukins (IL-6) noticed in mice brain following compromise of BBB after JEV inoculation via tail vein

IL-6: The level of IL-6 was slightly decreased at 1 day post infection and was almost similar with increasing time points post infection. Although there was a decrease but this decrease wasnot significant (Fig. 9a) when compared to the level expressed at 0 day (the value was normalized to 100%) post JEV infection. When we compared the levels expressed between days, we noticed a non-significant slight decrease among the day post JEV infection. Overall we noticed a non significant slight decrease in IL6 level in mice brain post JEV infection via tail vein at almost all time points compared to 0dpi. Hence, no significant change in IL-6 Ievel was noticed with disease progression at later stage of infection (Fig. 9a).

Upregulated expression of interleukins (IL-17, IL-21) noticed in mice brain following compromise of BBB after JEV inoculation via tail vein

IL-17: The level of IL-17 was significantly increased with increasing time points post infection. At 3 day post infection (dpi), the IL-17 level increased to 197% (p< 0.0011) which increased significantly at 5dpi (291%, p=0.0002) and reached to the level 392% (p<0.0001) at 7 dpi post infection (Fig. 10a) when compared to the level expressed at 0 day (the value was normalized to 100%) post JEV infection. When we compared the levels expressed between days, we noticed a significant 146%, p=0.0035 increase in IL-17 level at 5dpi compared to 3 day post JEV infection. At 7 dpi 135% (p=0.0029) increase was noticed compared to 5 day post infection. Overall we noticed an increase in IL-17 level in mice brain post JEV infection via tail vein at later days of infection compared to 0dpi. Hence, the IL-17 level increased with disease progression at later stage of infection (Fig. 10a).

IL21: The level of IL21 significantly increased with increasing time points post infection when compared to 0 day post infection (dpi). At 1 day post infection (dpi), the IL21level drastically increased to 404% (p<0.0001) which increased significantly at 3dpi (435%, p<0.0001), 5dpi (619%, p<0.0001) and reached to the level 789% (p<0.0001) at 7dpi post infection (Fig. 11a) when compared to the level expressed at 0 day (the value was normalized to 100%) post JEV infection. When we compared the levels expressed between days, we noticed a significant 142%, p=0.0048 increase in IL21 level at 5dpi compared to 3 day post JEV infection. At 7dpi the level was significantly increased by 127%, p=0.0006 was compared to 5day post infection. Overall we noticed an increase in IL-21 level in mice brain post JEV infection via tail vein at later days of infection compared to 0 dpi. Hence, the IL21 level was increased with disease progression at later stage of infection (Fig. 11a).

Upregulated expression of chemokines (MCP-1) noticed in mice brain following compromise of BBB after JEV inoculation via tail vein

MCP1: The level of MCP1 increased with increasing time points post infection. At 3 day post infection (dpi) the MCP1 level increased to 143% (p=0.0161) which increased significantly at 5dpi (192%, p=0.0007) and reached to the level 248% (p<0.0001) at 7dpi post infection (Fig. 12a) when compared to the level expressed at 0 day (the value was normalized to 100%) post JEV infection. When we compared the levels expressed between days we noticed a significant 137%, (p=0.00165) increase in MCP1 level at 3dpi compared to 1day post JEV infection. A significant 134%, p = 0.0082 increase at 5dpi was noticed compared to 3 day post infection. At 7dpi, the level significantly increased by 248%, p =0.0031 compared to 5 day post infection. Overall we noticed an increase in MCP-1 level in mice brain post JEV infection via tail vein at later days of infection compared to 0 dpi. Hence, the MCP1 level increased with disease progression at later stage of infection (Fig. 12a).

Down-regulated expression of chemokines (RANTES) were noticed in mice brain following compromise of BBB after JEV inoculation via tail vein

RANTES: The level of RANTES significantly decreased with increasing time points post infection. At 1 day post infection (dpi), the RANTES level was decreased to 25% (p= 0.0085) which decreased significantly at 3dpi (35%, p=0.0066), 5dpi(23%, p=0.0007) and reached to the level 21 % (p=0.0002) at 7dpi post infection (Fig. 13a) when compared to the level expressed at 0 day (the value was normalized to 100%) post JEV infection.

When we compared the levels expressed between days, we noticed a 72%, p= 0.0041 decrease in RANTES level at 3dpi compared to 1day post JEV infection but this decrease was not significant. At 5dpi the level was almost similar to the level expressed at 3 day post infection.

Similarly, at 7dpi, the level was almost similar to the level expressed at 5 day post infection. Overall we noticed a decrease in RANTES level in mice brain post JEV infection via tail vein at later days of infection compared to 0 dpi. Hence, the RANTES level was decreased with disease progression at later stage of infection (Fig. 13a).

Down-regulated expression of IFN-ϒ and FOXP3+ noticed in mice brain following compromise of BBB after JEV inoculation via tail vein

IFN-ϒ: The level of IFN-ϒ decreased at later time points post infection. At 5 day post infection (dpi), the IFN-ϒ level decreased significantly to 64%, p=0.0015which decreased significantly to 38%, p< 0.0001 at 7dpi (Fig. 14a) when compared to the level expressed at 0 day (the value was normalized to 100%) post JEV infection. When we compared the levels expressed between days, we noticed a significant 59%, p= 0.0049 decrease in IFN-ϒ level at 7dpi compared to 5 day post JEV infection. Overall we noticed a decrease in IFN-ϒ level in mice brain at later days post infection compared to 0dpi. Hence, the IFN-ϒ level decreased with disease progression at later stage of infection (Fig. 14a).

FOXP3+: No significant decrease in the level of FOXP3+ was noticed when compared to the level expressed at 0 day (the value was normalized to 100%) post JEV infection. Similarly, when we compared the levels expressed between days, no significant decrease in FOXP3+ level was noticed (Fig. 15a). Overall we noticed no significant decrease in FOXP3+level in mice brain at any points post infection compared to 0dpi. Hence, no significant change in the FOXP3+level was noticed with disease progression at later stage of infection (Fig. 15a).

Expression levels of TLRs (TLR-2, TLR-4, TLR-9), interleukins (IL-6, IL-17, IL-21), chemokines (MCP-1, RANTES), IFN-ϒ and FOXP3+ in mice brain following JEV inoculation via IC route. Upregulated expression of TLRs (TLR-2, TLR-4, TLR-9) noticed in mice brain following JEV inoculation via IC route

TLR2: The level of TLR2 significantly increased with increasing time points post infection when compared to 0 day post infection (dpi). At 1 day post infection (dpi), the TLR2 level increased to 381% (p<0.0001) which increased significantly at 3dpi (1524%, p<0.0001), 5dpi (1800%, p<0.0001) and reached to the level 3178% (p<0.0001) at 7dpi post infection (Fig. 6b) when compared to the level expressed at 0 day (the value was normalized to 100%) post JEV infection. When we compared the levels expressed between days, we noticed a significant 400%, p<0.0001 increase in TLR 2 level at 3dpi compared to 1day post JEV infection. Only118% increase at 5dpi was noticed compared to 3 day post infection. At 7dpi, the level was significantly increased by 177%, p<0.0001 was compared to 5day post infection. Overall we noticed an increase in TLR2 level in mice brain at later days post infection compared to 0dpi. Hence, the TLR2 level increased with disease progression at later stage of infection (Fig. 6b).

TLR4: The level of TLR4 significantly increased with increasing time points post infection when compared to 0 day post infection (dpi). At 1dpi, the TLR4 level increased to 169%(p=0.0085) which increased significantly at 3dpi (191%, p=0.0066), 5dpi (230%, p<0.0007) and reached to the level 262% (p<0.0002) at 7dpi (Fig. 7b) when compared to the level expressed at 0 day (the value was normalized to 100%) post JEV infection. When we compared the levels expressed between days, we noticed that although TLR 4 level increased at 3dpi compared to 1day post JEV infection, this increase was not significant. The 120% increase at 5dpi was noticed compared to 3 day post infection. At 7dpi, the level increased slightly compared to 5day post infection. But those increases in TLR 4 levels were not significant. Overall we noticed an increase in TLR4 level in mice brain at later days post infection compared to 0dpi. Hence, the TLR4 level increased with disease progression at later stage of infection (Fig. 7b).

TLR9: The level of TLR9 significantly increased with increasing time points post infection when compared to 0 day post infection (dpi). At 1 dpi, the TLR9 level increased to 154% (p=0.0095) which increased significantly at 3dpi (181%, p=0.0041), 5dpi (325%, p<0.0003) and reached to the level 602% (p<0.0001) at 7dpi (Fig. 8b) when compared to the level expressed at 0 day (the value was normalized to 100%) post JEV infection. When we compared the levels expressed between days, we noticed a significant 179% (p=0.0013) increase in TLR9 levels at 5dpi compared to 3 day post infection. At 7dpi, the level significantly increased by 185%, p<0.0001 was compared to 5day post infection. Overall we noticed an increase in TLR9 level in mice brain at later days post infection compared to 0dpi. Hence, the TLR9 level increased with disease progression at later stage of infection (Fig. 8b).

Upregulated expression of interleukins (IL-6, IL-17, IL-21) noticed in mice brain following JEV inoculation via IC route

IL-6: The level of IL-6 significantly increased with increasing time points post infection. There was a significant and marked upregulation in the level of IL-6 from 3 day post infection (dpi) 206% (p=0.0043) to 5dpi (1179%, p<0.0001) which reached to the level 2599% (p<0.0001) at 7dpi post infection (Fig. 9b) when compared to the level expressed at 0 day (the value was normalized to 100%) post JEV infection. When we compared the levels expressed between days, we noticed a significant 574%, p<0.0001 increase in IL-6 level at 5dpi compared to 3 day post JEV infection. At 7dpi, the level significantly increased by 220%, p=0.02 was compared to 5day post infection. Overall we noticed an increase in IL-6 level in mice brain at later days post infection compared to 0dpi. Hence, the IL-6 level increased with disease progression at later stage of infection (Fig. 9b).

IL-17: The level of IL-17 significantly increased with increasing time points post infection. At 3 day post infection (dpi), the IL-17 level increased to 124% ($p<0.0001$) which increased significantly at 5dpi (806%, $p<0.0001$) and reached to the level 971% ($p<0.0001$) at 7dpi post infection (Fig. 10b) when compared to the level expressed at 0 day (the value was normalized to 100%) post JEV infection. When we compared the levels expressed between days, we noticed a significant 650%, $p<0.0001$ increase in IL-17 level at 5dpi compared to 3 day post JEV infection. Only120% ($P=0.0013$) increase at 7dpi was noticed compared to 5 day post infection. Overall we noticed an increase in IL-17 level in mice brain at later days post infection compared to 0dpi. Hence, the IL-17 level increased with disease progression at later stage of infection (Fig. 10b).

IL21: The level of IL21 significantly increased at later time points post infection. Only219% increase at 5dpi ($p< 0.0047$) was noticed and at 7dpi, the level robustly increased by 875%, $p<0.0001$ when compared to the level expressed at 0 day (the value was normalized to 100%) post JEV infection. A significant 165% ($p < 0.0221$) increase in IL21 level at 5dpi was noticed compared to 3 day post JEV infection (Fig. 11b). When we compared the levels expressed between days, we noticed a significant 400% increase at 7 dpi compared to 5 day post infection. Overall we noticed a robust increase in IL21 level in mice brain at later day 7 post infection compared to 0dpi. Hence, the IL21 level significantly enhanced with disease progression at later stage of infection (Fig. 11b).

Upregulated expression of chemokines (MCP-1 and RANTES) noticed in mice brain following JEV inoculation via IC route

MCP1: The level of MCP1 significantly increased with increasing time points post infection. At 3 day post infection (dpi) the MCP1 level increased to 259% ($p=0.0007$) which increased significantly at 5dpi (639%, $p<0.0001$) and reached to the level 1188% ($p<0.0001$) at 7dpi post infection (Fig. 12b) when compared to the level expressed at 0 day (the value was normalized to 100%) post JEV infection. When we compared the levels expressed between days, we noticed a significant 156%, $p= 0.0041$ increase in MCP1 level at 3dpi compared to 1day post JEV infection. A significant 246%, $p<0.0001$ increase at 5dpi was noticed compared to 3 day post infection. At 7dpi, the level significantly increased by 187%, $p<0.0001$ compared to 5day post infection. Overall we noticed an increase in MCP1 level in mice brain with increasing time points post infection which robustly increased during later stages of JEV infection compared to 0dpi. Hence, the MCP1 level increased with disease progression at later stage of infection (Fig. 12b).

RANTES: The level of RANTES significantly increased with increasing time points post infection. At 1 day post infection (dpi), the RANTES level increased to 958% ($p= 0.0076$) which increased significantly at 3dpi (3091%, $p=0.0007$), 5dpi (4653%, $p<0.0001$) and reached to the level 5930 % ($p<0.0001$) at 7dpi post infection (Fig 13b) when compared to the level expressed at 0 day (the value was normalized to 100%) post JEV infection. When we compared the levels expressed between days, we noticed a significant 323%, $p= 0.0041$ increase in RANTES level at 3dpi compared to 1day post JEV infection. A 151%, $p<0.0001$ increase at 5dpi was noticed compared to 3 day post infection. At 7dpi, the level was significantly increased by 127%, $p<0.0001$ compared to 5day post infection. Overall we noticed a exaggerated increase in RANTES level in mice brain with increasing time points post infection compared to 0dpi. Hence, the RANTES level increased with disease progression which significantly upregulated dramatically at later stage of infection (Fig. 13b).

Down-regulated expression of IFN-ϒ noticed in mice brain following JEV inoculation via IC route

IFN-ϒ: The level of IFN-ϒ decreased significantly with increasing time points post infection. At 3day post infection (dpi), the IFN-ϒ level decreased significantly to 46%, $p=0.0056$ which decreased significantly at 5dpi (41%, $p=0.0047$) and finally decreased to the level 24% ($p=0.0015$) at 7dpi post infection (Fig. 14b) when compared to the level expressed at 0 day (the value was normalized to 100%) post JEV infection. When we compared the levels expressed between days we noticed a significant 54%, $p=0.0025$decrease in IFN-ϒ level at 3dpi compared to 1day post JEV infection. The IFN-ϒ level was further decreased significantly to 59%, $p =0.0294$ at 7 dpi compared to 5day post infection. Overall we noticed a decrease in IFN-ϒ level in mice brain at later days post infection compared to 0dpi. Hence, the IFN-ϒ level decreased with disease progression at later stage of infection (Fig 14b).

Up-regulated expression of FOXP3+ noticed in mice brain following JEV inoculation via IC route

FOXP3+: The level of FOXP3+ significantly increased with increasing time points post infection. At 3 day post infection (dpi), the FOXP3+ level increased to 197% ($p=0.0002$) which increased significantly at 5dpi (348%, $p<0.0001$) and reached to the level 863% ($p<0.0001$) at 7dpi post infection (Fig. 15b) when compared to the level expressed at 0 day (the value was normalized to 100%) post JEV infection. When we compared the levels expressed between days, we noticed a significant 168 %, $p= 0.0012$ increase in FOXP3+ level at 3dpi compared to 1day post JEV infection. An increase in 177%, $p =0.0005$ at 5dpi was noticed compared to 3 day post infection. At 7dpi, the level significantly increased by 248%, $p =0.0247$ compared to 5day post infection. Overall we noticed an increase in FOXP3+levelin mice brain at later days post infection compared to 0dpi. Hence, the FOXP3+level increased with disease progression at later stage of infection (Fig. 15b).

Discussion

Viral CNS infections result in exacerbated inflammation responsible for several symptoms such as fever, headache, confusion, stroke, seizure, or death[12]. Such infections trigger

reactivity of resident immune and glial cells that serve as defenses for the CNS, namely, microglia and astrocytes. This results in the release of proinflammatory cytokines and subsequent activation of both innate and adaptive immune responses. When acute, this neuroinflammatory response is necessary and even beneficial to the neural environment in eliminating pathogens or aiding brain repair. However, when extreme threats to the neural environment such as protein aggregates accumulate in the brain and protractedly sustain inflammation, continuous gliosis and apoptosis can occur as a result of unregulated inflammatory cytokine release.

Microglia is the primary non-neuronal innate sensors of viral infections in the central nervous system (CNS)[9]. Past studies proposed the polarization of microglia into proinflammatory M1 microglia, which are CD14-, CD16-, CD32-, CD40-, CD86-, MHC-II-, translocator protein- and inducible nitric oxide synthase-positive and anti-inflammatory M2 microglia expressing CD163, CD206, Arg1 and other markers[18]. In the context of viral encephalitis, it has been shown, for instance, that upon west nile virus (WNV) infection of the CNS, microglia are activated and display upregulation of certain M1-like markers such as Iba-1, as well as chemokines such as CCL2, CCL3, CCL5 and CCL7[38].

In contrast, treatment with the anti-inflammatory drug minocycline reduced the expression of M1-like markers and increased the expression of M2-like markers. Such M2-like microglia were associated with neuroprotective effects in WNV infection of the CNS[39], suggesting that M1-like microglia are needed for the initial control of WNV infection whereas M2-like microglia prevent excessive tissue damage during CNS inflammation.

Viruses have evolved several strategies to evade host immune detection and clearance. Chemokines are involved in the mobilization and guidance of effector cells to sites of inflammation. A plethora of immune and resident CNS cells can produce both chemokines and chemokine receptors during neuroinflammation, thereby modulating the local inflammatory milieu. These cells include granulocytes, lymphocytes, monocytes but also resident neurons, endothelial cells and in particular microglia and astrocytes. They survey the CNS parenchyma, respond to viral stressors and regulate the egress of viral particles across brain regions.

Cytokines are critical mediators of inflammation. Neurotropic flaviviruses, including Japanese encephalitis, are able to participate in the body's immune response through the TLR signaling pathway.Role of cytokines interferon-gamma (IFN-γ) and tumour necrosis factor (TNF) are implicated in JEV pathogenesis.

- TNF has been detected in MS lesions[16,42] and TNF levels in cerebrospinal fluid correlated with disease progression in MS patients[43]. In EAE, TNF is up-regulated early by microglia before the onset of clinical symptoms and is expressed later by T cells and macrophages. It has been demonstrated that TNF plays an important role in regulation of immune cell infiltration in EAE[3,29]. Studies have reported that TNF-α, can regulate the expression of chemokine/chemokine receptors and other adhesion molecules by endothelial cells of the brain and they can enhance the trafficking and the homing of inflammatory leukocytes to the brain, leading to an exacerbated disease profile[25,36].
- Studies on EAE in rodents have shown that inhibition or a lack of IFN-γ exacerbates EAE and can make resistant strains susceptible to disease[11]. IFNγ was shown to contribute to protection from CNS infection[21]. In contrast, targeting of IFNγ with a neutralizing antibody improved BBB integrity in one study, suggesting its role in enhancing BBB permeability[22].
- Studies have shown that TLRs have an important role in mediating inflammation and immune response to the JE virus. Transcriptome profile study[13] in the JEV infected mice brain showed an increased expression of mRNAs of TLR2, TLR3 and TLR7.
- Our previous study[45] investigated the role of all cytokines, chemokines and TLRs in JEV infection *in vitro*, using a mouse neuroblastoma Neuro2a cell line as well as in microglia cell line BV2. We noticed a robust increase in cytokines (IL-6 and IL-17), chemokines (MCP-1 and RANTES), TLR 2, 4 and 9 expression in both BV2 and Neuro 2A cell lines at later time point post infection. These findings suggest that cytokines, chemokines and TLRs have a critical role in immunopathogenesis of JEV infection. Thus keeping our *in vitro* observations in mind, we decided to expand our study to determine the role of cytokines, chemokines and TLRs *in vivo* mouse model of encephalitis by infecting BALB/c mice with JEV through the intracerebral route.

  The cascade events that result following JEV infection in vitro as well as *in vivo* have not been identified. Therefore, this study was designed to investigate the role of all PRRs in JEV infection with special emphasis on understanding the role of TLRs and other PRRs in JEV infection in vitro using mouse neuronalcell line and compare with events that occur *in vivo* using JEV-infected suckling and adult mice. The experimental paradigm for tail vein and IC JEV infection to study TLRs, cytokines and chemokines expression is given in fig. 1.
- We noticed microglial activation in mice brain following JEV infection. This was confirmed by estimating the levels of Iba-1 in the mice brain at different time points post JEV infection. After JEV infection, the expression of Iba-1 was significantly upregulated, suggesting that microglia were activated in virus-infected brain (Fig. 5). Hence, it is confirmed that the upregulated expression of Iba-I level in mouse brain was due to JE virus infection. Activated microglia may contribute to neuronal damage.

Earlier studies have reported microglial activation following JEV infection resulting in the release of tumor necrosis factor α (TNF-α), IL-1β, IL-6, monocyte chemoattractant protein-1 (MCP-1), chemokine (C-C motif) ligand 5 (CCL5), CXC motif chemokine ligand 10 (CXCL10) and inducible nitric oxide synthase, which may be related to endothelial barrier damage[8,33]. In earlier studies following viral infection in CNS, the significant role of Iba-I was observed in regulating some immunological and pathophysiological functions of microglia during virus infection in mouse brain[27]. CNS-infiltrating immune cells in JEV-infected mice brain have been noticed in earlier studies[37].

- Role of TLRs in flavivirus-mediated immune responses has been demonstrated earlier. TLR4 knockout mice showed increased resistance to JEV infection[14]. The loss of TLR4 caused powerful type I IFN responses in dendritic cells and macrophages via greater stimulation of antiviral IFN-stimulated genes via distinct activation of IFN regulating factor 3 and nuclear factor kappa-light-chain-enhancer of activated B cells (NF-κB)[14].
- We noticed upregulated expression of TLRs (2, 4 and 9) in both tail vein and IC infected mice groups at later stages of infection (5 and 7 dpi) compared to 0 dpi (Figures 6, 7 and 8). The age and sex matched control/mock infected (pbs inoculation) were also included. No changes in expression of TLRs were noticed at any stage of infection compared to 0 dpi in mock infected (pbs inoculation) group both via tail vein and IC inoculation.
- Mice affected with JEV show a high amount of cytokine and chemokine production in the brain[5]. Inflammation due to JEV amplifies BBB breakdown. IL-6 plays a crucial role in altering the permeability of BBB to facilitate JEV entry. Il-6 digests the BBB's tight junctions leading to CNS inflammation[6,7,20].
- We noticed upregulated expression of IL-6 following JEV infection in mice via IC route with disease progression. No change in IL-6 level was noticed at any time points compared to 0dpi (Fig. 9). A 5 to maximum 10-fold increase in TNFα, IL1α and IL6 mRNA expression was found at 7 and 10 dpi in the CNS of pigs infected with JEV[40]. IL-6 is the main cytokine including IL-1β and TNF-α which influences BBB structure and function in inflammation. Studies have shown that blocking pro-inflammatory cytokines, TNF-α, IL-1β and IL-6 can reduce the permeability of BBB and can improve the outcome of neurological diseases and injuries to great extent[52].

- IL-17 up-regulates antiapoptotic molecules and consequently, increases persistent infection by enhancing the survival of virus-infected cells and blocking target cell destruction by cytotoxic T cells. Neutralization of IL-17 augments virus clearance by eliminating virus-infected cells and boosting lytic function by cytotoxic T cells, leading to the prevention of disease development. Studies have shown that IL-17 plays a pivotal role in mediating different types of tissue inflammation and destruction in chronic toxoplasmic encephalitis[47], experimental autoimmune encephalitis[46], human multiple sclerosis[4] and psoriasis[35]. Th17 cells and their cytokine IL-17 play a critical role in the pathogenesis of TMEV-induced chronic demyelinating disease[17].

  The elimination of IL-17 function from TMEV-infected mice appears to prevent the development of demyelinating disease[17]. The production of IL-17 has been reported during HIV infection in humans[23,30,53] and herpes simplex virus[26]and respiratory syncytial virus infections[15] in rodents.

  We observed increased levels of IL-17 at all dpi compared to 0dpi in both teil vein and IC route infected mice groups. The levels of IL-17 were increased with disease progression (Fig. 10). Hence, our finding suggests that expression of IL-17 might play detrimental role following JEV infection.

- IL-21, an essential cytokine for the induction and maintenance of Th17 cells, has the potential to suppress the production of IFN-γ by T lymphocytes and to drive cytotoxic $CD8^+$ T cells to apoptosis[1,19,31,32]. We observed increased levels of IL-21 at all dpi compared to 0dpi in both teil vein and IC route infected mice groups. The levels of IL-21 were increased with disease progression (Fig. 11). Hence, our finding suggests expression of IL-21 might play detrimental role following JEV infection. In contrast to IL-21, we observed dramatic decrease in IFN- γ level in both teil vein and IC route infected mice groups at all dpi compared to 0dpi (Fig. 14).

  Neutralization of IFN-γ ameliorated the disruption of BBB integrity and the downregulation of TJ proteins[22]. It has been demonstrated that treatment with an anti-IFN-γ antibody significantly decreased the uptake of NaF compared to isotype control, indicating that blocking IFN-γ can ameliorate the disruption of BBB integrity[22]. Also, the expression of occludin, claudin-5 and ZO-1 decreased less in the brains of mice treated with anti-IFN-γ antibody compared to those treated with the isotype control[22].

- Chemokine expression in the infected CNS is often regulated by cytokine production via infiltrating leukocytes. Infection by several different viruses has been correlated with a rapid induction of chemokines from astrocytes and microglia. MCP-1 (Monocyte chemoattractant protein-1), also known as Chemokine (CC-motif) ligand 2 (CCL2), is from family of CC chemokines. It has a vital role in the process of inflammation where it attracts or enhances the expression of other inflammatory factors/cells. The

role of MCP-1 has been implicated in pathogenesis of various diseases where it contributes by numerous mechanisms. Increased mRNA expression of MCP-1 (CCL2) and RANTES (CCL5) leads to an infiltration of macrophages and activated T cells[6,7,20].

We observed increased levels of MCP-1 at all dpi compared to 0dpi in both teil vein and IC route infected mice groups. The levels of MCP-1 increased with disease progression (Fig. 12). We noticed a drastic increase in the level of RANTES in IC route infected mice groups (Fig. 13). We noticed a significant decrease in RANTES level via teil vein injected mice group. Inflammatory cytokines or chemokines (IL-6, IFN-γ, CXCL10 and CCL2 to CCL5) can deteriorate BBB permeability via downregulation of the TJ proteins claudin-5, occludin and ZO-1[41].

Conclusion

In summary, in our study we observed that JEV infection causes microglial activation as a result of which proinflammatory cytokines (TNF-α, IL-6, IL-17, IL-21), chemokines (MCP-1, RANTES) were upregulated, which may be related to endothelial barrier damage[8,33]. Thus, elevated levels of inflammatory cytokines and chemokines, high viral titers in the brain and fatalities caused by JE can all be connected.

Hence, we can say that increased expressions of proinflammatory cytokines and chemokines in our study were associated with increased tissue damage and death at later stages of infection. The understanding of the pathogenetic mechanisms leading to immune-mediated tissue damage during the course of JEV is important to develop novel treatment strategies to prevent detrimental effects of the immune response.

Acknowledgement

We wish to thank Dr. Sudhanshu Vrati for giving us JEV strain GP-78.

References

1. Barker B.R., Parvani J.G., Meyer D., Hey A.S., Skak K. and Letvin N.L., IL-21 induces apoptosis of antigen-specific CD8+ T lymphocytes, *J Immunol*., **179(6)**, 3596-603 **(2007)**

2. Baker R.G., Hayden M.S. and Ghosh S., NF-κB, inflammation and metabolic disease, *Cell Metab*., **13(1)**, 11-22 **(2011)**

3. Barten D.M. and Ruddle N.H., Vascular cell adhesion molecule-1 modulation by tumor necrosis factor in experimental allergic encephalomyelitis, *J Neuroimmunol*., **51(2)**, 123-33 **(1994)**

4. Bettelli E., Oukka M. and Kuchroo V.K., T(H)-17 cells in the circle of immunity and autoimmunity, *Nat Immunol*., **8(4)**, 345-50 **(2007)**

5. Biswas S.M., Kar S., Singh R., Chakraborty D., Vipat V., Raut C.G., Mishra A.C., Gore M.M. and Ghosh D., Immunomodulatory cytokines determine the outcome of Japanese encephalitis virus infection in mice, *J Med Virol*., **82(2)**, 304-10 **(2010)**

6. Chen C.J., Chen J.H., Chen S.Y., Liao S.L. and Raung S.L., Upregulation of RANTES gene expression in neuroglia by Japanese encephalitis virus infection, *J Virol*., **78(22)**, 12107-19 **(2004)**

7. Chen C.J., Ou Y.C., Lin S.Y., Raung S.L., Liao S.L., Lai C.Y., Chen S.Y. and Chen J.H., Glial activation involvement in neuronal death by Japanese encephalitis virus infection, *J Gen Virol*., **91(Pt 4)**, 1028-37 **(2010)**

8. Chen T. et al, Research advancements in the neurological presentation of flaviviruses, *Rev Med Virol*., **29(1)**, e2021 **(2021)**

9. Chen Z., Zhong D. and Li G., The role of microglia in viral encephalitis: a review, *J Neuroinflammation*, **16(1)**, 76 **(2019)**

10. Daniels B.P. et al, Regional astrocyte IFN signaling restricts pathogenesis during neurotropic viral infection, *J Clin Invest*., **127(3)**, 843-856 **(2017)**

11. Ferber I.A. et al, Mice with a disrupted IFN-gamma gene are susceptible to the induction of experimental autoimmune encephalomyelitis (EAE), *J Immunol*., **156(1)**, 5-7 **(1996)**

12. Furr S.R. and Marriott I., Viral CNS infections: role of glial pattern recognition receptors in neuroinflammation, *Front Microbiol*., **3**, 201 **(2012)**

13. Gupta N. and Rao P.V., Transcriptomic profile of host response in Japanese encephalitis virus infection, *Virol J*., **8**, 92 **(2011)**

14. Han Y.W., Choi J.Y., Uyangaa E., Kim S.B., Kim J.H., Kim B.S., Kim K. and Eo S.K., Distinct dictation of Japanese encephalitis virus-induced neuroinflammation and lethality via triggering TLR3 and TLR4 signal pathways, *PLoS Pathog*., **10(9)**, e1004319 **(2014)**

15. Hashimoto K. et al, Respiratory syncytial virus infection in the absence of STAT 1 results in airway dysfunction, airway mucus and augmented IL-17 levels, *J Allergy ClinImmunol*., **116(3)**, 550-7 **(2005)**

16. Hofman F.M., Hinton D.R., Johnson K. and Merrill J.E., Tumor necrosis factor identified in multiple sclerosis brain, *J Exp Med*., **170(2)**, 607-12 **(1989)**

17. Hou W., Kang H.S. and Kim B.S., Th17 cells enhance viral persistence and inhibit T cell cytotoxicity in a model of chronic virus infection, *J Exp Med*., **206(2)**, 313-28 **(2009)**

18. Jurga A.M., Paleczna M. and Kuter K.Z., Overview of General and Discriminating Markers of Differential Microglia Phenotypes, *Front Cell Neurosci*., **14**, 198 **(2020)**

19. Korn T. et al, IL-21 initiates an alternative pathway to induce proinflammatory T(H)17 cells, *Nature*, **448(7152)**, 484-487 **(2007)**

20. Lannes N., Summerfield A. and Filgueira L., Regulation of inflammation in Japanese encephalitis, *J Neuroinflammation*., **14(1)**, 158 **(2017)**

21. Larena M., Regner M. and Lobigs M., Cytolytic effector pathways and IFN-γ help protect against Japanese encephalitis, *Eur J Immunol*., **43(7)**, 1789-98 **(2013)**

22. Li F. et al, Viral Infection of the Central Nervous System and Neuroinflammation Precede Blood-Brain Barrier Disruption during Japanese Encephalitis Virus Infection, *J Virol*., **89(10)**, 5602-14 **(2015)**

23. Maek-A-Nantawat W., Buranapraditkun S., Klaewsongkram J. and Ruxrungtham K., Increased interleukin-17 production both in helper T cell subset Th17 and CD4-negative T cells in human immunodeficiency virus infection, *Viral Immunol*., **20(1)**, 66-75 **(2007)**

24. Misra U.K. and Kalita J., Overview: Japanese encephalitis, *Prog Neurobiol*., **91(2)**, 108-20 **(2010)**

25. Miu J. et al, Chemokine gene expression during fatal murine cerebral malaria and protection due to CXCR3 deficiency, *J Immunol*., **180(2)**, 1217-30 **(2008)**

26. Molesworth-Kenyon S.J., Yin R., Oakes J.E. and Lausch R.N., IL-17 receptor signaling influences virus-induced corneal inflammation, *J Leukoc Biol*., **83(2)**, 401-8 **(2008)**

27. Mori I., Imai Y., Kohsaka S. and Kimura Y., Upregulated expression of Iba1 molecules in the central nervous system of mice in response to neurovirulent influenza A virus infection, *Microbiol Immunol*., **44(8)**, 729-35 **(2000)**

28. Mosser D.M. and Edwards J.P., Exploring the full spectrum of macrophage activation, *Nat Rev Immunol*., **8(12)**, 958-69 **(2008)**

29. Murphy C.A., Hoek R.M., Wiekowski M.T., Lira S.A. and Sedgwick J.D., Interactions between hemopoietically derived TNF and central nervous system-resident glial chemokines underlie initiation of autoimmune inflammation in the brain, *J Immunol*., **169(12)**, 7054-62 **(2002)**

30. Ndhlovu L.C., Chapman J.M., Jha A.R., Snyder-Cappione J.E., Pagán M., Leal F.E., Boland B.S., Norris P.J., Rosenberg M.G. and Nixon D.F., Suppression of HIV-1 plasma viral load below detection preserves IL-17 producing T cells in HIV-1 infection, *AIDS*, **22(8)**, 990-2 **(2008)**

31. Nurieva R. et al, Essential autocrine regulation by IL-21 in the generation of inflammatory T cells, *Nature*, **448(7152)**, 480-3 **(2007)**

32. Palmer M.T. and Weaver C.T., Immunology: narcissistic helpers, *Nature*, **448(7152)**, 416-8 **(2007)**

33. Pardridge W.M., Drug transport across the blood-brain barrier, *J Cereb Blood Flow Metab*., **32(11)**, 1959-72 **(2012)**

34. Paun A. and Pitha P.M., The innate antiviral response: new insights into a continuing story, *Adv Virus Res*., **69**, 1-66 **(2007)**

35. Pène J. et al, Chronically inflamed human tissues are infiltrated by highly differentiated Th17 lymphocytes, *J Immunol*., **180(11)**, 7423-30 **(2008)**

36. Pober J.S. and Sessa W.C., Evolving functions of endothelial cells in inflammation, *Nat Rev Immunol*., **7(10)**, 803-15 **(2007)**

37. Qi L. et al, VEGFR-3 signaling restrains the neuron-macrophage crosstalk during neurotropic viral infection, *Cell Rep*., **42(5)**, 112489 **(2023)**

38. Quick E.D., Leser J.S., Clarke P. and Tyler K.L., Activation of intrinsic immune responses and microglial phagocytosis in an ex vivo spinal cord slice culture model of West Nile virus infection, *J Virol*., **88(22)**, 13005-14 **(2014)**

39. Quick E.D., Seitz S., Clarke P. and Tyler K.L., Minocycline Has Anti-inflammatory Effects and Reduces Cytotoxicity in an *Ex Vivo* Spinal Cord Slice Culture Model of West Nile Virus Infection, *J Virol*., **91(22)**, e00569-17 **(2017)**

40. Redant V. et al, Efficient control of Japanese encephalitis virus in the central nervous system of infected pigs occurs in the absence of a pronounced inflammatory immune response, *J Neuroinflammation*, **17(1)**, 315 **(2020)**

41. Roe K., Kumar M., Lum S., Orillo B., Nerurkar V.R. and Verma S., West Nile virus-induced disruption of the blood-brain barrier in mice is characterized by the degradation of the junctional complex proteins and increase in multiple matrix metalloproteinases, *J Gen Virol*., **93(Pt 6)**, 1193-1203 **(2012)**

42. Selmaj K., Raine C.S., Cannella B. and Brosnan C.F., Identification of lymphotoxin and tumor necrosis factor in multiple sclerosis lesions, *J Clin Invest*., **87(3)**, 949-54 **(1991)**

43. Sharief M.K. and Hentges R., Association between tumor necrosis factor-alpha and disease progression in patients with multiple sclerosis, *N Engl J Med*., **325(7)**, 467-72 **(1991)**

44. Sharma A., Bhomia M., Honnold S.P. and Maheshwari R.K., Role of adhesion molecules and inflammation in Venezuelan equine encephalitis virus infected mouse brain, *Virol J*., **8**, 197 **(2011)**

45. Shukla M., Garg A., Dhole T.N. and Chaturvedi R., Exaggerated levels of some specific TLRs, cytokines and chemokines in Japanese encephalitis infected BV2 and neuro 2A cell lines associated with worst outcome, *Virol J*., **20(1)**, 16 **(2023)**

46. Steinman L., A brief history of T(H)17, the first major revision in the T(H)1/T(H)2 hypothesis of T cell-mediated tissue damage, *Nat Med*., **13(2)**, 139-45 **(2007)**

47. Stumhofer J.S. et al, Interleukin 27 negatively regulates the development of interleukin 17-producing T helper cells during chronic inflammation of the central nervous system, *Nat Immunol*., **7(9)**, 937-45 **(2006)**

48. Tang Y. and Le W., Differential Roles of M1 and M2 Microglia in Neurodegenerative Diseases, *Mol Neurobiol*., **53(2)**, 1181-1194 **(2016)**

49. Turtle L., Griffiths M.J. and Solomon T., Encephalitis caused by flaviviruses, *QJM*, **105(3)**, 219-23 **(2012)**

50. Turtle L. and Solomon T., Japanese encephalitis—the prospects for new treatments, *Nature Reviews Neurology*, **14(5)**, 298-313 **(2018)**

51. Wei R., Li X., Wang X., Zhang N., Wang Y., Zhang X., Gong P. and Li J., *Trypanosomaevansi* evades host innate immunity by

releasing extracellular vesicles to activate TLR2-AKT signaling pathway, *Virulence*, **12(1)**, 2017-2036 **(2021)**

52. Yang J., Ran M., Li H., Lin Y., Ma K., Yang Y., Fu X. and Yang S., New insight into neurological degeneration: Inflammatory cytokines and blood-brain barrier, *Front Mol Neurosci*., **15**, 1013933 **(2022)**

53. Yue F.Y., Merchant A., Kovacs C.M., Loutfy M., Persad D. and Ostrowski M.A., Virus-specific interleukin-17-producing CD4+ T cells are detectable in early human immunodeficiency virus type 1 infection, *J Virol.*, **82(13)**, 6767-71 **(2008)**

54. Zhao G., Gao Y., Zhang J., Zhang H., Xie C., Nan F., Feng S., Ha Z., Li C., Zhu X., Li Z., Zhang P., Zhang Y., Lu H. and Jin N., Toll-like receptor 2 signaling pathway activation contributes to a highly efficient inflammatory response in Japanese encephalitis virus-infected mouse microglial cells by proteomics, *Front Microbiol.*, **13**, 989183 **(2022)**.

(Received 09th September 2024, accepted 28th October 2024)